

Optimization of used cottonseed oil methyl ester production using response surface methodology

Abdullateef Jimoh*, Sani Uba, Victor .O. Ajibola, Edith .B. Agbaji

Department of Chemistry, Ahmadu Bello University, Zaria, Kaduna State, Nigeria

*Correspondence: Jimoh Abdullateef, Department of Chemistry, Kogi State College of Education, Ankpa, Kogi State, Nigeria.

ARTICLE INFO

Article history:

Received 29 August 2022

Received in revised form 7 September 2022

Accepted 5 November 2022

Available online 2 April 2023

Keywords:

Monoalkyl ester
 Transesterification
 Vegetable oil
 Biodiesel
 Free Fatty Acids

ABSTRACT

Biodiesel is the term for used cottonseed oil (UCSO), animal fat, and vegetable oil monoalkyl ester. Because of its similar and compatible fuel properties to diesel fuel, biodiesel obtained from UCSO is becoming more and more significant as an alternative fuel for use in diesel engines. The amount of free fatty acids (FFA) determines how biodiesel is produced from oil. In this study, the titration method was used to determine the FFA values of crude cottonseed oil (CCSO) and UCSO. These values were measured to be 0.56 % and 1.26 %, respectively. Heterogeneous alkali catalyzed transesterification is used to convert UCSO into biodiesel. It includes mixing methanol with UCSO in the presence of heterogeneous catalysts that is blend calcined, hydrated, and dehydrated eggshells and coconut shells CaO. The methanol-oil ratio, reaction temperature, reaction time, and catalyst concentration were the reaction factors that control the transesterification process. The Box-Behnken Design Response Surface Methodology was used to optimize the aforementioned parameters. Plots of the response surface and contour have been made among numerous factors that affect the production of biodiesel. A 1:10 molar ratio, 2.5 wt. % catalyst concentration, 80 minutes of reaction time, and a reaction temperature of 60 °C result in an optimum UCSO methyl ester yield of 93.60 %. The experimental yield, which was calculated after the optimized yield, was found to be 94.50 % based on these parameters, thus showing the effectiveness of the Response Surface Methodology as a tool for optimizing yield of biodiesel produced.

1. Introduction

The majority of the rising energy demands of the world are fueled by nonrenewable resources including coal, petroleum, and natural gas [1]. The lack of readily available fossil fuels necessitates the search for alternatives. Among the many alternative energy sources, biodiesel is more apparent for use in diesel engines [2]. The majority of biodiesel comes from vegetable oils; however, they have higher viscosity and cold flow properties than other sources. Continuous use of vegetable oils in engines can lead to issues like injector blockage and decreased performance. Through the transesterification process, viscosity-related issues can be reduced. In the presence of catalysts like KOH,

growth leads to increased fuel consumption, especially for cooking oils, which are harmful to the environment if improperly discarded after use [1]. Used cooking oil (UCO) is a viable and affordable feedstock for the synthesis of biofuels due to its low cost and extensive availability [4]. UCO, such as frying oil used once or multiple times, can be converted into biodiesel. Finding the optimal production settings will result in biodiesel from UCO and vegetable oils with similar fuel properties [5]. It is discovered that UCO contains significant levels of free fatty acids (FFAs), which can be reduced using an alkali-based transesterification procedure [6]. Alkali transesterification was found to occur utilizing a heterogeneous catalyst, CaO [7]. When the acid value of the UCO is less than 2 %, there is no

need for pretreatment, and the transesterification reaction initiated by the alkali-based procedure is sufficient to transform the UCO into methyl ester [8]. The methanol-oil ratio, catalyst concentration, reaction temperature, and

*Corresponding author. Tel: +234-803-800-5793; E-mail: abjijmoh@abu.edu.ng
 CaO, or NaOH, the triglycerides in vegetable oils react with alcohol to produce biodiesel [3]. Rapid population

reaction duration are only few of the variables that affect how much biodiesel may be produced from the feedstock. Changing one of the operational parameters with the function of time is a labour-intensive and expensive method of optimizing the production of biodiesel. Furthermore, the multivariate analysis process cannot be looked at concurrently. Nonlinear methods like a neural network, fuzzy logic, and experiment design can be used to investigate the combined effect of input parameters for multivariate situations [9]. The most effective method for multivariate analysis of the biodiesel production process with improved error control and in a variety of circumstances is response surface methodology (RSM) [10]. RSM is a potent statistical tool for examining how various independent variables affect the dependent variable. So, through optimization, RSM increases productivity and lowers the time, material, and cost associated with a lot of trials [11]. RSM offers a variety of response surface designs, however BBD (Box Behnken Design) is more labour-efficient and works well for fitting second-order polynomial equations with three or more experimental components [12]. However, because the catalyst cannot be reused and must be neutralized after the reaction, biodiesel cannot compete satisfactorily with fossil fuels. The processes required to produce biodiesel can be homogeneously catalyzed to generate large yields in a relatively short period of time [13]. The search for solid catalysts that are eco-friendly and effective is as a result of environmental concerns [14]. The chemical process used to produce biodiesel relies on the solid in the system catalyzing the reaction to shorten the time and cost of the process by reusing the catalyst, limit the number of contaminants in the reaction products, and carry out the operation in a continuous fixed bed [15]. Studies have shown that burning biodiesel (100%) reduces greenhouse gas emissions, making it perfect for usage in sensitive situations [7]. The heterogeneous solid-state catalyst and the effectiveness of the transesterification process are connected. Further research is needed to establish the optimum temperature and time for each reaction, as a heterogeneous catalyst often offers a better conversion efficiency than a homogeneous catalyst [16]. Because of its inexpensive cost of production and high basicity, calcium oxide (CaO) has previously been used in research investigations as a heterogeneous catalyst [7]. [17] used CaO as a heterogeneous catalyst in an oil transesterification reaction, achieving a 95 % conversion of the oil to the ester using a methanol to oil molar ratio of 12:01, 8 wt. % CaO with the oil mass, and a 3-hour reaction period. [18] performed the same reaction and, using CaO as the catalyst and 5% catalyst to oil (m/m), achieved 93 % conversion in 80 minutes at a reaction temperature of 65°C. The authors employed a 6:1 molar ratio of methanol to oil. [19] employing *Jatropha curcas* oil and a blend of CaO/ammonium carbonate solution, 93 %

conversion was attained. [20] carried out a comparable investigation employing a catalyst made of CaO and lithium doped. Due to the greater production ratio with conventional methods based on bench reactors, all of the tests by the authors previously mentioned for the production of biodiesel in continuum processes were carried out in a fixed-bed reactor on a laboratory scale [7]. The main issue for a technological, industrial, social, and economic development of a nation is energy sources and how to use them properly. Our energy needs have been met by natural wood resources for the past five generations, or more than a century [21]. Wood, however, lost its status as the main fuel as a result of the quick decline in the cost of fossil fuels and their wide spread accessibility. In a similar vein, the need for legislation to limit emissions and cut fuel consumption rates is growing stronger by the day [22]. The use of renewable or bio-based fuels, such as diesel blended with biodiesel, is a workable short - to mid-term strategy for resolving the issues. Due to the benefits of having a high cetane number and being self-sustaining, biodiesel is becoming a viable alternative fuel for diesel engines [23]. Moreover, emissions from burning fossil fuels such as unburned hydrocarbons (HC), oxides of carbon monoxide (CO_x), oxides of nitrogen (NO_x), particulate matters (PM), and organic gases have a negative impact on the environment and living things [24]. However, compared to diesel fuel, biodiesel has significant drawbacks, including greater viscosity, higher pour point, hygroscopic propensity, lesser volatility, and poorer cold flow property [25]. Sunflower (*Helianthus annuus*), soy bean (*Glycine max*), cottonseed (*Gossypium hirsutum*), linseed (*Linum usitatissimum*), mahua (*Madhuca longifolia*), jatropha (*Jatropha curcas*), pongamia (*Millettia pinnata*), among other plant species, are some examples of the various types of biodiesel fuels [22]. Furthermore, the transesterified vegetable oils or biofuels can be appropriately adjusted before being used in a diesel engine by heating them or mixing them with other biodiesel fuels, etc. The results of these studies show that when all the parameters are optimized, particularly the molar ratio, reaction temperature, catalyst concentration, and reaction time, the conversion of vegetable oil to biodiesel through transesterification using alkali supported on calcium oxide (NaOH/CaO) blend from calcined waste eggshell and coconut shell as a heterogeneous catalyst provides a maximum conversion of 94 % in the production of biodiesel. For these experiments, a bench reactor on a hot plate with a mechanical agitator and reflux condenser was used. This study uses used cottonseed oil (UCSO) as fuel and an alkali calcined-hydrated-dehydrated CaO (C_H_D-CaO) heterogeneous catalyst synthesized from an eggshell-coconut husk blend in order to analyze the impact of operational parameters on the biodiesel production process. The third goal is to determine the optimum molar

ratios, reaction temperatures, reaction times, and catalyst concentrations that increase UCSO biodiesel yield.

Experimental Methodology, Materials and Chemicals

Inorganic scums were filtered out of 10 L of used cottonseed oil samples that were purchased from a local eatery in Funtua, Katsina state, Nigeria. By using a colour indication titration method in accordance with ASTM D974 guidelines, the FFA contents of the UCSO samples were determined. The UCSO was discovered to have an acid value of 2.52 % and an FFA value of 1.26 %, indicating that the pretreatment step is not necessary for the oil because its FFA value is under 2.5 %. The transesterification process has a 3 % FFA limit because, above this level, the reaction step undergoes hydrolysis, producing soap and water, which lowers the ester yield [26]. Methanol (99.8 % purity), isopropyl alcohol, and other reagents used in this work were analytical grade chemicals that were purchased from British Drug House Ltd (BDL), UK, and Sigma-Aldrich. These chemicals were necessary for the transesterification process.

Catalyst Preparation

The eggshell and coconut husk wastes were properly washed in tap water to get rid of any unwanted material that had clung to their surfaces, then rinsed twice in distilled water before being dried for 24 hours in a hot air oven at 100 °C. Once it had been crushed, the powder was sieved. The eggshell powder and coconut husk powder were both set at 250 µm in size. The leftover dry eggshell and coconut husk materials were then calcined separately at 800 °C for 4 hours in a muffle furnace with static air at a heating rate of 2.5 °C/min. To prevent reactions with carbon dioxide (CO₂) and humidity air before use, all calcined samples were stored in a closed desiccator [27]. The previously calcined CaO-blend of coconut husk and eggshell waste were then subjected to hydration reaction in a reflux condenser containing water for 6 hours at 60 °C, after which filtered and dried in an oven for an entire night at 120 °C, calcined again for 3 hours at 600 °C (dehydration), and then stored in a desiccator to prevent oxidation. UCSO, methanol, and the catalyst were thereafter combined to perform the transesterification process. Prior to both of them receiving the aforementioned procedures, 1 g of solid coconut waste and 5 g of the eggshell were added [28].

Characterizations of Catalysts

Gas chromatogram-mass spectroscopy (GC-MS) analysis was used to assess the fatty acid composition of the crude, refined, and synthetic biodiesel (UCSOME). The general properties of these samples, including acid number, viscosity, density, and flash point were determined. The presence of a functional group in the calcined-hydrated-dehydrated CaO-blend was determined using Fourier Transform Infrared (FTIR) spectroscopy (Perkin Elmer

1000 spectrometer; Perkin Elmer, Waltham, MA, USA), and the functional group present in commercial CaO was compared. Using a scanning electron microscope (SEM) (ZEISS EVO LS10 operating at 20kV), the surface morphology of the synthesized catalyst was examined. EDS analysis (JEOLJSM-600F) was used to determine the elements that were present in the synthesized catalyst whereas, X-ray diffraction (XRD) analysis (XRD Rigacu MiniFlex 300) was used to confirm that the synthesized catalyst produced was calcium oxide (CaO) [27].

Experimental Design and Statistical Analysis

As a response to the transesterification reaction of UCSO samples, the current work focuses on a four-level Box-Behnken Design (BBD) in response surface methodology (RSM) to improve the percentage yield of UCSOME, the molar ratio, reaction temperature, catalyst concentration, and reaction time were chosen as the independent variables for the analysis. Software for statistical analysis was used to establish the importance of each element, interaction, and quadratic term in the optimization process [Design expert software version 11.0.0 Stat ease, Minneapolis, USA]. Each factor was varied at three different levels -1, 0, and +1 signifying low, medium, and high values. The arrangement of the factorial design is shown in Table 1. A total of 27 experiments were employed in this work to evaluate the effects of the four main independent factors on the percentage yield of UCSOME production. A non-linear regression method was used to fit the second-order polynomial (Eq. (1)) to the experimental data and to identify the relevant model terms. Considering all the linear terms, square terms, and linear by linear interaction items, the quadratic response model can be described as Eq. (1):

$$\text{Yield} = \beta_0 \pm \sum_{i=1}^n \beta_i X_i \pm \beta_{ii} X_i^2 \pm \sum_{i=1}^{n-1} \sum_{j=i+1}^n \beta_{ij} X_i X_j \quad (1)$$

Where; Yield represents an objective to optimize the response as a percentage of used cottonseed oil methyl ester yield, β_0 = constant-coefficient, β_i = regression coefficient of the linear terms, β_{ii} = regression coefficient of the quadratic terms, β_{ij} = regression coefficient of the interaction terms, and X_i and X_j are independent variables [29].

Transesterification of UCSO

The transesterification reaction methanol to oil molar ratio in mol/mol, reaction temperature in °C, CaO concentration in units of wt.%, and reaction duration in min were all subjected to an optimization design consisting of 27 runs. A 500 cm³ three-necked round-bottomed flask with a reflux condenser was used to conduct the transesterification reaction. A mechanical stirrer running at an appropriate rotation rate per minute (rpm) was used to stir the mixture. Each experiment used 50 g of UCSO reactants with the addition of an alkali

calcined-hydrated-dehydrated CaO-blend as heterogeneous catalyst. The Gallenhamp magnetic stirrer hot plate was used to warm the reaction flask. After the reaction period, the mixture was placed into a 75 cm³ sample tube for further centrifugation for 15 minutes. The ester and trace glycerol layers were separated by transferring the top layer into a separating funnel. Glycerol, surplus methanol, and other products were removed from the lower layer of the mixture. To get rid

of the remnants of the catalyst, methanol, and glycerol, the top layer of the methyl ester was scraped off and washed with phosphoric acid (0.1 wt. %) and distilled water. The methyl ester was washed repeatedly up until the finished product pH solution becomes neutral. To remove the moisture content, the product was finally heated to 100°C [30-31].

Table 1: Range of Process Variables for Box Behnken Design

Factor	Parameter	Units	Low	Medium	High
A	Molar ratio	mol/mol	1:10	1:10.4	1:10.8
B	Reaction temperature	°C	50	55	60
C	Reaction time	min	50	80	110
D	Catalyst Concentration	wt.%	1.0	2.5	4.0

Table 2: Experimental Box Behnken Design (BBD) matrix with the Results of Response

Std	Run	Factor 1	Factor 2	Factor 3	Factor 4	Response
		A: Methanol/Oil ratio (wt.%)	B: Reaction Temperature (°C)	C: Reaction Time (min)	D: Catalyst Conc. (wt.%)	UCSOME yield (%)
2	1	10.8	50	80	2.5	91.3
22	2	10.4	60	80	1	92.1
26	3	10.4	55	80	2.5	92.2
6	4	10.4	55	110	1	90.0
27	5	10.4	55	80	2.5	92.3
24	6	10.4	60	80	4	93.2
9	7	10	55	80	1	78.4
14	8	10.4	60	50	2.5	93.2
3	9	10	60	80	2.5	93.6
20	10	10.8	55	110	2.5	83.2
23	11	10.4	50	80	4	85.4
17	12	10	55	50	2.5	77.4
1	13	10	50	80	2.5	78.3
5	14	10.4	55	50	1	90.1
8	15	10.4	55	110	4	92.2
25	16	10.4	55	80	2.5	92.3
4	17	10.8	60	80	2.5	84.2
21	18	10.4	50	80	1	82.1
15	19	10.4	50	110	2.5	84.4
7	20	10.4	55	50	4	91.3
16	21	10.4	60	110	2.5	84.2
10	22	10.8	55	80	1	82.1
11	23	10	55	80	4	80.4
18	24	10.8	55	50	2.5	82.3
19	25	10	55	110	2.5	80.4
13	26	10.4	50	50	2.5	81.2
12	27	10.8	55	80	4	85.3

The yield of biodiesel is calculated by Eq. (2);

$$\text{Biodiesel Yield (\%)} = \frac{(\text{mass of biodiesel produced in grams})}{(\text{mass in grams of raw oil taken for reaction})} \times 100 \quad (2)$$

Results and Discussion

Model fitting

BBD model analysis

BBD designed a total of 27 experiments (runs) (Table 2). The BBD technique was used to analyze the individual and combined effects of the four variables under consideration on the UCSOME yield (as a response): A: molar ratio, B: reaction temperature, C: catalyst concentration, and D: reaction time. The mathematical formulation of the link between the response and the process variables was performed using a quadratic polynomial model. The results of the ANOVA tests were assessed for significance of the regression model for the response, and Table 4 displays the findings. Model term values $\text{Prob}>F<0.0500$ indicates that certain conditions make some factors significant. A, B, C, AD, BC, CD, A^2 , B^2 , C^2 , and D^2 are important model parameters for response (%UCSOME yield). D-reaction time, AC, AB, and BD were discovered to have less of an impact on the percentage of UCSOME production efficiency than the other parameters. The following Eq. (3) presents the empirical relationships between the tested factor and response:

$$\text{UCSOME YIELD} = +92.43 - 1.32A + 1.79B - 1.64C - 0.4775D + 1.55AB - 0.9AC - 4.26AD + 4.88BC + 0.655BD + 2.95CD - 24.37A^2 - 7.16B^2 - 7.73C^2 - 3.34D^2 \quad (3)$$

A positive sign in Eq. (3) indicates a synergistic effect of the factors, while a negative sign indicates an antagonistic effect of the factors [32]. ANOVA analysis for response factors indicates that the value of R-squared (determination coefficient) is 0.9953 which is very high and reveals a good correlation between the actual and the predicted values as shown in Fig. 8 (predicted vs actual plot).

Analysis of variance (ANOVA)

The original second-order quadratic model that BBD constructed (shown in Equation-3) and the most important factors in converting UCSO to biodiesel are evaluated by BBD ANOVA analysis, which is displayed in Table-3. Before displaying any collected results, a satisfactory validation must be completed. The mole ratio (A), reaction temperature (B), and reaction duration (C) are very significant characteristics, as indicated by the p-value of the model which was less than 0.0001. According to the regression analysis, a significant model is one with a p-value of 0.0001 or higher. Three linear terms (A, B, and C), three cross-product interaction terms (AD, BC, and CD), and four quadratic terms (A^2 , B^2 , C^2 , and D^2) imply that the variables have a considerable impact on UCSOME yield [33-34]. The F-value from the ANOVA analysis, which is found to be 204.95 for a model, 30.51 for the reaction temperature (B), 57.55 and 75.37 for the two cross-product interaction terms AD and BC, respectively, and 2510.42, 216.84, 252.9, and 47.28 for the four quadratic terms (A^2 , B^2 , C^2 , and D^2), respectively, determines the performance of the yield response. High F-value of reaction temperature and catalyst concentration indicates that they are the experimental conditions that have the greatest impact on the conversion of UCSO to biodiesel (UCSOME). A $p>0.005$ indicates that the lack of fit, which is used to test the applicability of the model, is not significant, indicating that there is less error between experimental data and results predicted by BBD research.

Table 3: ANOVA for the Quadratic Model Regression

Analysis of Variance for Values						
Source	DF	SEQ SS	ADJ SS	ADJ MS	F	p-value prob>F
Regression	14	3619.2	3619.2	258.51	204.95	<0.0001
Linear	4	0.9625	0.9625	23.603	18.71	<0.0001
square	4	3307.67	3307.67	826.92	655.59	<0.0001
Interaction	6	217.12	217.12	36.187	28.69	<0.0001
Residual	12	15.14	15.14	1.26		
Lack of Fit	10	12.85	12.85	1.28	1.12	0.5591
Pure Error	2	2.29	2.29	1.14		
Cor Total	26	3634.33				

Term Coefficient						
Source	Sum of Squares	df	Mean Square	F-value	p-value	
Model	3619.2	14	258.51	204.95	< 0.0001	significant

A-MOLAR RATIO	20.88	1	20.88	16.56	0.0016	significant
B-REACTION TEMPERATURE	38.49	1	38.49	30.51	<0.0001	significant
C- REACTION TIME	32.31	1	32.31	25.61	0.0003	significant
D- CATALYST CONCENTRATION	2.74	1	2.74	2.17	0.1665	Insignificant
AB	9.64	1	9.64	7.64	0.0171	Insignificant
AC	3.24	1	3.24	2.57	0.135	Insignificant
AD	72.59	1	72.59	57.55	< 0.0001	significant
BC	95.06	1	95.06	75.37	< 0.0001	significant
BD	1.72	1	1.72	1.36	0.2661	Insignificant
CD	34.87	1	34.87	27.64	0.0002	significant
A ²	3166.48	1	3166.48	2510.42	< 0.0001	significant
B ²	273.51	1	273.51	216.84	< 0.0001	significant
C ²	318.99	1	318.99	252.9	< 0.0001	significant
D ²	59.63	1	59.63	47.28	< 0.0001	significant

Characterization of Catalyst

Figure 14 displays the FTIR spectra of commercial CaO and blended calcined-hydrated-dehydrated CaO in the range of 450-4000 cm⁻¹. The bottom spectrum is a spectrum of commercial CaO (COMM_CaO), while the top spectrum is the spectrum of derived blended calcined-hydrated-dehydrated CaO (C_H_D-CaO) catalyst. The bands in the spectrum at 3638.99 cm⁻¹ and 3642.23 cm⁻¹ representing O-H stretching vibrations of Ca(OH)₂ can be attributed to the presence of the signals detected over the two catalysts. Since the surface of the pellets for commercial and blended CaO absorbs moisture from an atmosphere that is coupled to the Ca atom [35]. While the peak between 1406.21 cm⁻¹ and 1430.33 cm⁻¹ is the result of the Ca-O stretching bending vibration. Very minute vibrations were detected at 2509.36cm⁻¹ in the blended CaO structure, which can be attributed to the sample CaCO₃ composition [36]. Similar to this, vibrations at 1420, 1085, and 577 cm⁻¹ bands were seen in the structure of the blended CaO, which may be related to the conversion of carbonate to CaO [37]. In addition, the CaO spectra of the sample show bands at 1396.84, 873.99, and 712.42 (for commercial CaO) and 1406.21, 873.07, and 712.28 (for calcined-hydrated-dehydrated CaO), respectively, which correspond to the stretching vibration of the CO₃²⁻ group found over the two catalysts and can be attributed to the chemisorption of gaseous CO₂ from the atmosphere over the surface of the catalyst [38]. Additional evidence for the production of CaO throughout the calcination-hydration-dehydration process of the eggshell and coconut husk waste mixture

was indicated by the stretching vibration mode of the Ca-O bond, which was observed at 528 cm⁻¹. More specifically, the IR spectra reveal that both varieties of CaO catalyst share the same properties. As a result, it can be concluded that the derived CaO, which is a mixture of eggshell and coconut shell, has the same potential as commercial CaO to act as a heterogeneous catalyst in the production of biodiesel. Furthermore, the obtained XRD data were compared to the JCPDS card number 37-1497, and peaks for (C_H_D-CaO) were found at 2θ = 19°, 35°, 49°, and 63° in Fig. 13 [39]. The mean crystallite size of the (C_H_D-CaO) particles was assessed using equation given by Debye-Scherrer [40] and was found to be 111.30 nm.

$$d = K\lambda/\beta \cos \theta \quad (4)$$

Where; β = full-width at half-maximum (in radian) and θ = is the position of the maximum of the diffraction peak. K is defined as the so-called shape factor, which usually has a value of about 0.9; λ = the X-ray wavelength (1.5406 Å for Cu Kα).

The result shows that the (C_H_D-CaO) structure is a face-centered cubic phase. It was determined from the XRD pattern that calcium oxide crystallizes in cubic phase, similar to the results obtained by [41][42][43][44]. The results were equivalent to those obtained by [45-46]. Minor peaks of hexagonal shaped Ca(OH)₂ were detected at 29°, 30°, 48°, 65° and 72° which can be attributed to the (C_H_D-CaO) being exposed to ambient air before analysis. Peaks at 29.36° and 44° show the presence of CaCO₃ species with a rhombohedral structure [47]. Moreover, the (C_H_D-CaO) exhibits a maximum particle size reduction and a greater surface area, two important characteristics of heterogeneous catalysts. The (C_H_D-CaO) SEM image clearly shows regular particle morphologies with clusters of solid cubic crystals and a

discernible reduction in particle sizes, indicating larger surface area beneficial for the transesterification reaction as shown in fig. 15 [48]. Further analysis of the (C_H_D-CaO) composition of its elements led to the production of the EDX spectra shown in figure 15, where the two peaks of Ca (71.5 %) and O (28.5 %) serve as proof of the purity of the sample.

Reusability of the Commercial (C_H_D-CaO)

One of the important characteristics in industrial applications is the stability and reusability of catalysts. As a result, Fig. 12 shows the results of the six cycles of testing the reusability of the calcined-hydrated-dehydrated CaO (C_H_D- CaO) with 2.5 wt.% catalysts (based on oil weight), a methanol to oil ratio of 10:1, a reaction temperature of 60 °C, and a reaction period of 80 min. After each phase, the solid catalyst was filtered out of the reaction mixture, cleaned of any adsorbed stains with methanol, and then recalined at 600°C for further usage. The results show that for each of the six tested runs, a high biodiesel conversion of above 70% was achieved. In Fig. 12, the graph of reusability is shown. With a conversion of more than 70%, the catalyst can be employed up to six more times before the conversion starts to decline noticeably. Leaching of active species into the biodiesel phase was likely the intended cause of this loss of activity. The catalyst activity will decrease if some of the bulk CaO dissolves in the methanolic solution [49]. Due to the loss of active sites caused by the pore blockage of the catalyst, the catalyst became inactive [50]. SEM micrographs showed that the catalysts were coated with intermediates or products such as diglyceride, monoglyceride, glycerol, biodiesel, and others (Fig. 15). This reduced the contact between the catalyst and the reactant mixtures. Another study carried out by [51] showed that the lifetime of all solid base catalysts (NaOH/Al₂O₃, CaO, SrO, CaMgO, and CaZnO) is limited to two cycles. Besides, the reusability of waste capiz (*Amusium cristatum*) shell was 2 cycles before decreasing to an amount of 50% [52]. While chicken bones were applied by [53] and their reusability was 4 cycles. More work was put into enhancing its stability and properties. The cost of the catalyst and maintenance would be reduced because it was made from waste shells.

Effect of Operating Parameters on the Yield of UCSO Methyl Ester

Interaction effects on Response and Process Optimization

An investigation carried out to ascertain whether there was a significant interaction impact between each of the two independent components (as shown in Table 3). On the production efficiency of UCSOME, the interaction impact of the molar ratio (A) and catalyst concentration (D) was significant (p-value 0.0001 as determined from Table 3). Within the experimental range, the other two

independent factors, reaction temperature (B) at 55°C and reaction time (C) at 80 min were simultaneously maintained constant. Fig. 5a and b, respectively, show the 2D contour plots and 3D surfaces for the AD interaction. Increased biodiesel yield is indicated by a disagreement in the molar ratio at 2.2 wt. % catalyst concentration, but the divergence was not significant at any other catalyst concentration. The yield of biodiesel increases to a high (93%) before decreasing. Furthermore, as the molar ratio and catalyst concentration increase, the UCSOME yield marginally also increases. As the molar ratio further increases, the yield thereafter starts to decline. In general, a high molar ratio ensures the success of the reaction by increasing the rate of methyl ester production. However, the overloading of methanol would inactivate the catalyst and reverse the reaction since transesterification is a reversible reaction [54]. Hence the 3D response curve under this condition indicates a significant interaction effect between molar ratio and catalyst concentration on the UCSOME yield. On the production efficiency of UCSOME, the interaction impact of reaction temperature (B) and reaction time (C) was significant (p<0.0001 as determined from Table 3). Within the experimental range, the other two independent variables, the methanol/oil ratio of 10.4 and the catalyst concentration of 2.5 g, were simultaneously maintained constant. In Fig. 4a and b, respectively, the 3D surfaces and 2D contours plots for BC interaction are shown. As the reaction temperature and reaction time increased, so did the three-dimensional surface plot of the anticipated conversion of UCSO to UCSOME. This could be owing to the reduction in viscosity of the oil on increasing the temperature, which resulted in better mixing of oil with alcohol and faster separation of glycerol from biodiesel. This result agrees with those reported in the literature where higher reaction temperature and initial mixing of the immiscible reactants cause a higher production of biodiesel [55-56]. Also, it was discovered that the interaction effect of Reaction time (C) and Catalyst concentration (D) on UCSOME production efficiency was substantial (p = 0.0002). Within the boundaries of the experimental range, the other two independent factors; the reaction duration at 80 minutes and the 2.5 g catalyst concentration were simultaneously maintained constant. In Fig. 6a and b, respectively, the 3D surfaces and 2D contours plots for CD contact are shown. With increasing catalyst concentration and reaction time, the UCSOME yield increased. Then, because of the influence of the reversible reaction in transesterification, there was a minor decrease when the reaction period was too lengthy [57]. The catalyst concentration and reaction duration have a sizable interaction effect on the UCSOME yield, as shown by the 3D response curve. At extremely high and very low values of reaction time, the modification of catalyst concentration has a less noticeable impact on the production yield of UCSOME [29]. The statistics suggest

that the yield of biodiesel increases and then decreases when the amount of catalyst is increased up to a certain point [58]. In a similar study [59] said that a shorter reaction time would be needed to reach an equilibrium conversion if there was not enough catalyst present. More so, the impact of an increasing catalyst diminishes over a protracted reaction period. Based on [60] a study that supports this research, a high catalyst concentration and a medium reaction duration were selected for the best UCSOME yield. As stated by [60], a greater catalyst concentration might speed up the reaction. The reaction would not be complete, however, if less catalyst were employed for a shorter period of time. Conversely, the reaction might not finish when a lot of catalyst is used and the reaction time is short. Therefore, it is crucial to

establish the optimum reaction period for the selected catalyst concentration. Based on the pattern seen in the figures, a prolonged reaction time results in decreased catalyst activity, which lowers UCSOME yield for an extended reaction time [61]. The difference in percentage between the experimental value and the predicted value was found to be 0.84 %, which is within the permitted range of 5 %. As a result, it was discovered that the predicted value of UCSOME production closely followed the experimental value, demonstrating the high level of accuracy of the model [62]. The ASTM D6751 standards were used to determine the fuel viscosity, density, calorific value, cetane number, flash point, cloud point, and pour point in order to evaluate the property of the resulting biodiesel.

Design-Expert® Software
Factor Coding: Actual

UCSOME yield (%)
● Design points above predicted value
○ Design points below predicted value
77.4 93.6

X1 = A: Methanol/Oil ratio
X2 = B: Reaction Temperature

Actual Factors
C: Reaction Time = 80
D: Catalyst Conc. = 2.5

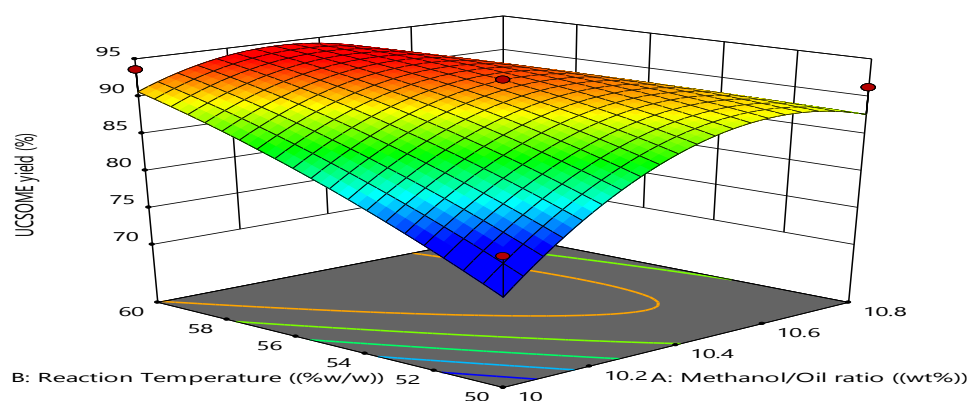


Figure 1a: Response surface plot between methanol/oil ratio and reaction temperature at reaction time 80 min and 2.5 g catalyst concentration

Design-Expert® Software
Factor Coding: Actual

UCSOME yield (%)
● Design Points
77.4 93.6

X1 = A: Methanol/Oil ratio
X2 = B: Reaction Temperature

Actual Factors
C: Reaction Time = 80
D: Catalyst Conc. = 2.5

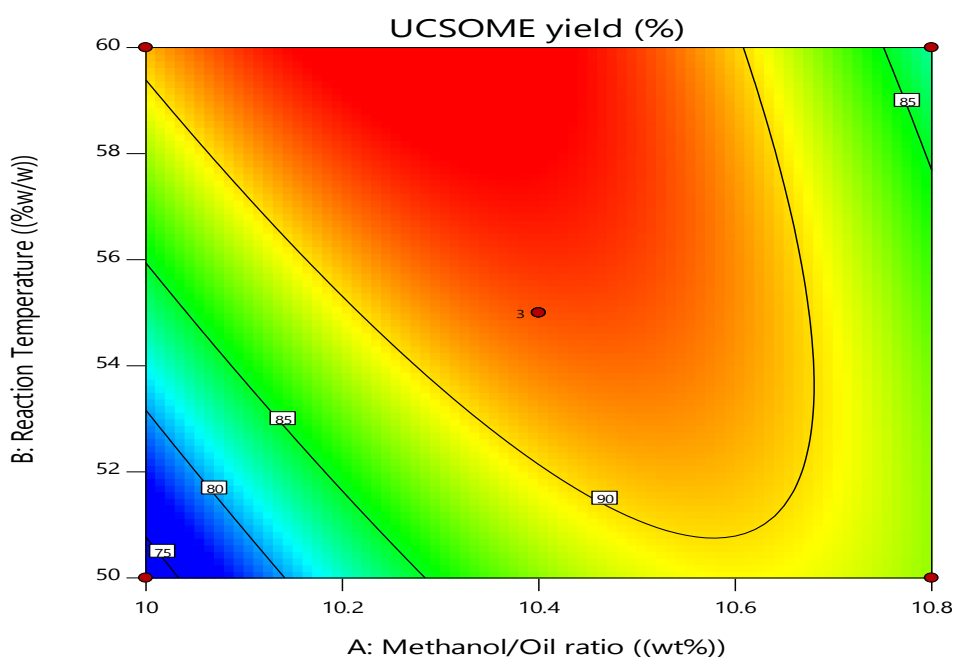


Figure 1b: Contour plot between methanol/oil ratio and reaction temperature at reaction time 80 min and 2.5 g catalyst concentration

Design-Expert® Software

Factor Coding: Actual

UCSOME yield (%)

● Design points above predicted value

○ Design points below predicted value

77.4 93.6

X1 = A: Methanol/Oil ratio

X2 = C: Reaction Time

Actual Factors

B: Reaction Temperature = 55

D: Catalyst Conc. = 2.5

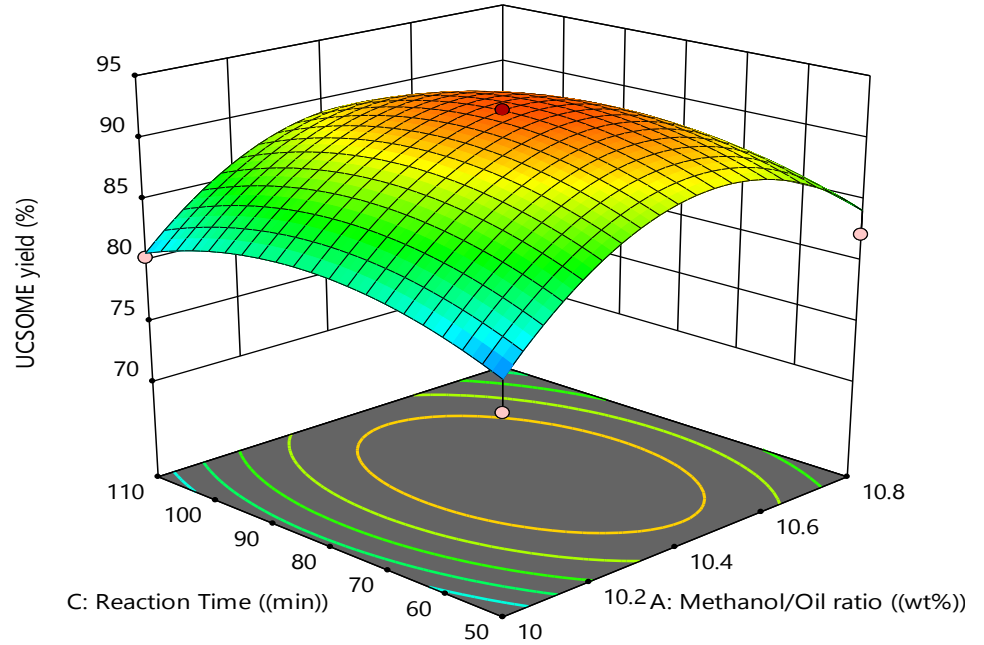


Figure 2a: Response surface plot between methanol/oil ratio and reaction time at reaction temperature 55°C and 2.5 g catalyst concentration

Design-Expert® Software

Factor Coding: Actual

UCSOME yield (%)

● Design Points

77.4 93.6

X1 = A: Methanol/Oil ratio

X2 = C: Reaction Time

Actual Factors

B: Reaction Temperature = 55

D: Catalyst Conc. = 2.5

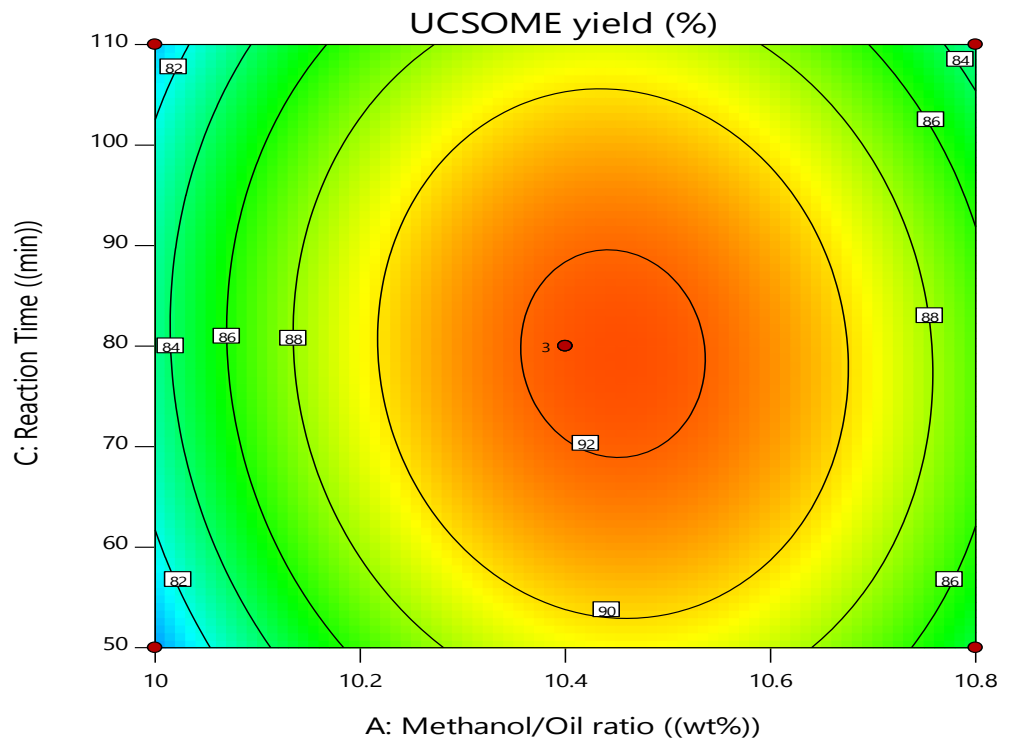


Figure 2b: Contour plot between methanol/oil ratio and at reaction temperature 55°C and 2.5 g catalyst concentration

Design-Expert® Software

Factor Coding: Actual

UCSOME yield (%)

● Design points above predicted value

○ Design points below predicted value

77.4 93.6

X1 = A: Methanol/Oil ratio

X2 = D: Catalyst Conc.

Actual Factors

B: Reaction Temperature = 55

C: Reaction Time = 80

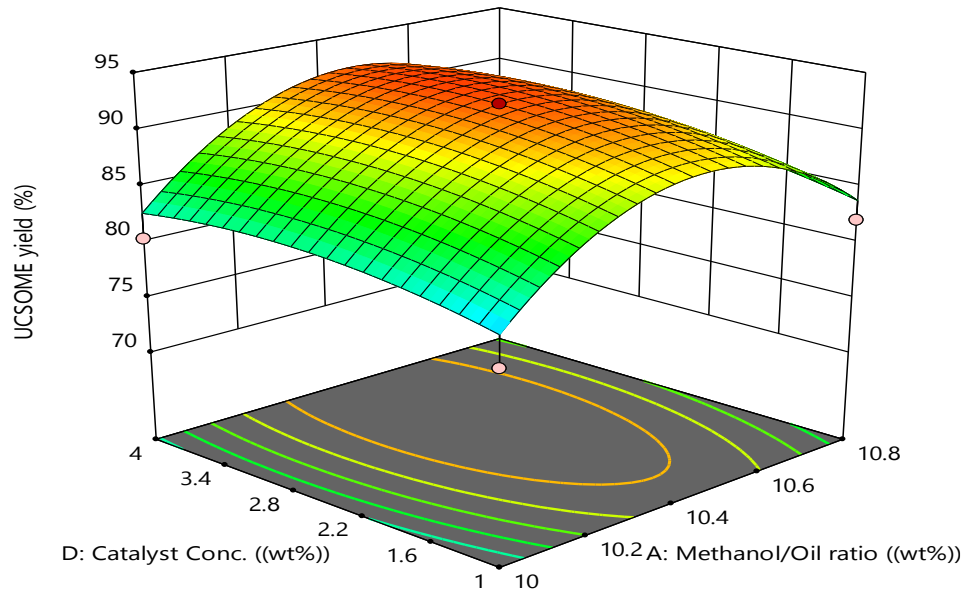


Figure 3a: Response surface plot between methanol/oil ratio and catalyst concentration at reaction temperature 55°C and 80 min reaction time

Design-Expert® Software

Factor Coding: Actual

UCSOME yield (%)

● Design Points

77.4 93.6

X1 = A: Methanol/Oil ratio

X2 = D: Catalyst Conc.

Actual Factors

B: Reaction Temperature = 55

C: Reaction Time = 80

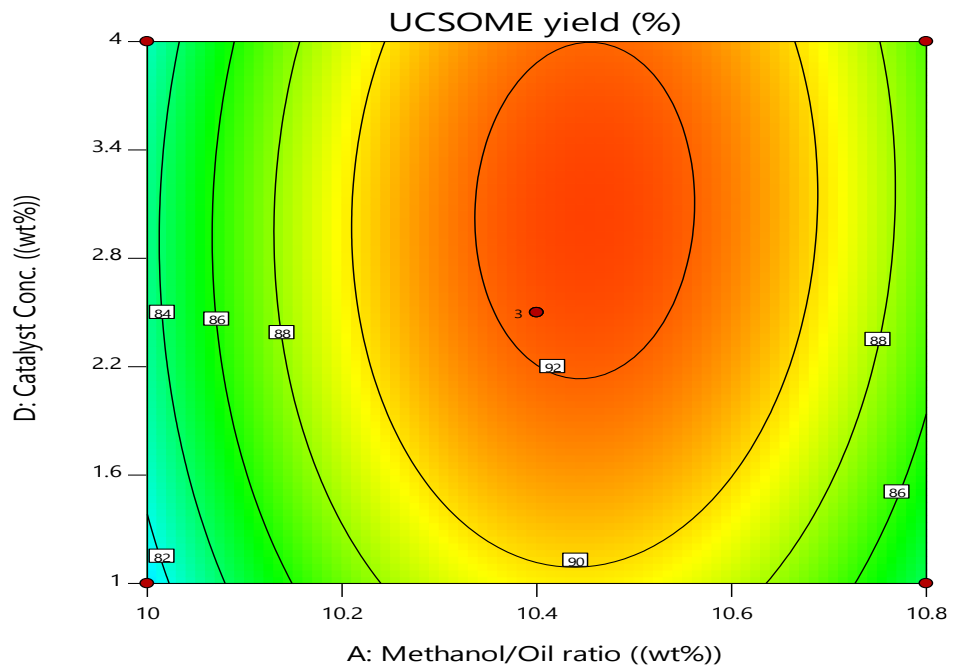


Figure 3b: Contour surface plot between methanol/oil ratio and catalyst concentration at reaction temperature 55°C and 80 min reaction time

Design-Expert® Software

Factor Coding: Actual

UCSOME yield (%)

● Design points above predicted value

○ Design points below predicted value

77.4 93.6

X1 = B: Reaction Temperature

X2 = C: Reaction Time

Actual Factors

A: Methanol/Oil ratio = 10.4

D: Catalyst Conc. = 2.5

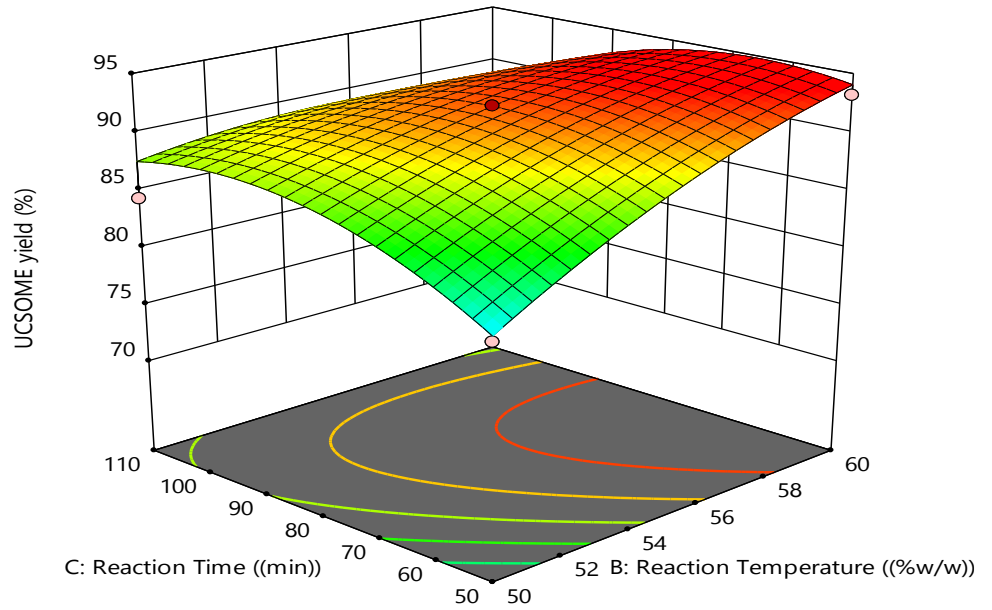


Figure 4a: Response surface plot between reaction time and reaction temperature at methanol/oil 10.4 and 2.5 g catalyst concentration

Design-Expert® Software

Factor Coding: Actual

UCSOME yield (%)

● Design Points

77.4 93.6

X1 = B: Reaction Temperature

X2 = C: Reaction Time

Actual Factors

A: Methanol/Oil ratio = 10.4

D: Catalyst Conc. = 2.5

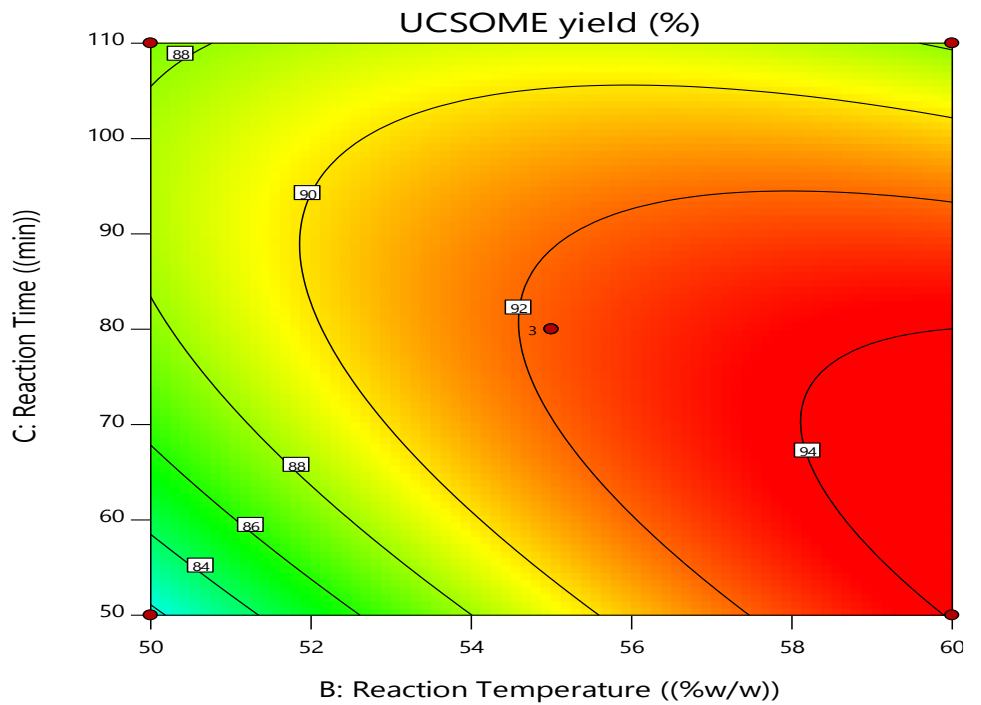


Figure 4b: Contour surface plot between reaction time and reaction temperature at methanol/oil ratio 10.4 and 2.5 g catalyst concentration

Design-Expert® Software

Factor Coding: Actual

UCSOME yield (%)

● Design points above predicted value

○ Design points below predicted value

77.4 93.6

X1 = B: Reaction Temperature

X2 = D: Catalyst Conc.

Actual Factors

A: Methanol/Oil ratio = 10.4

C: Reaction Time = 80

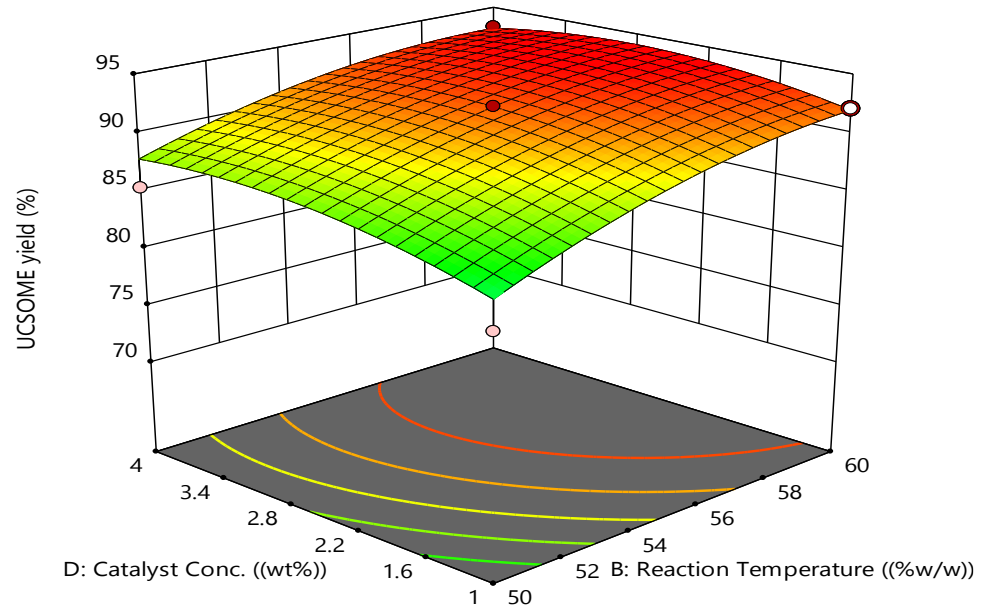


Figure 5a: Response surface plot between catalyst concentration and reaction temperature at methanol/oil ratio 10.4 and 80min reaction time

Design-Expert® Software

Factor Coding: Actual

UCSOME yield (%)

● Design Points

77.4 93.6

X1 = B: Reaction Temperature

X2 = D: Catalyst Conc.

Actual Factors

A: Methanol/Oil ratio = 10.4

C: Reaction Time = 80

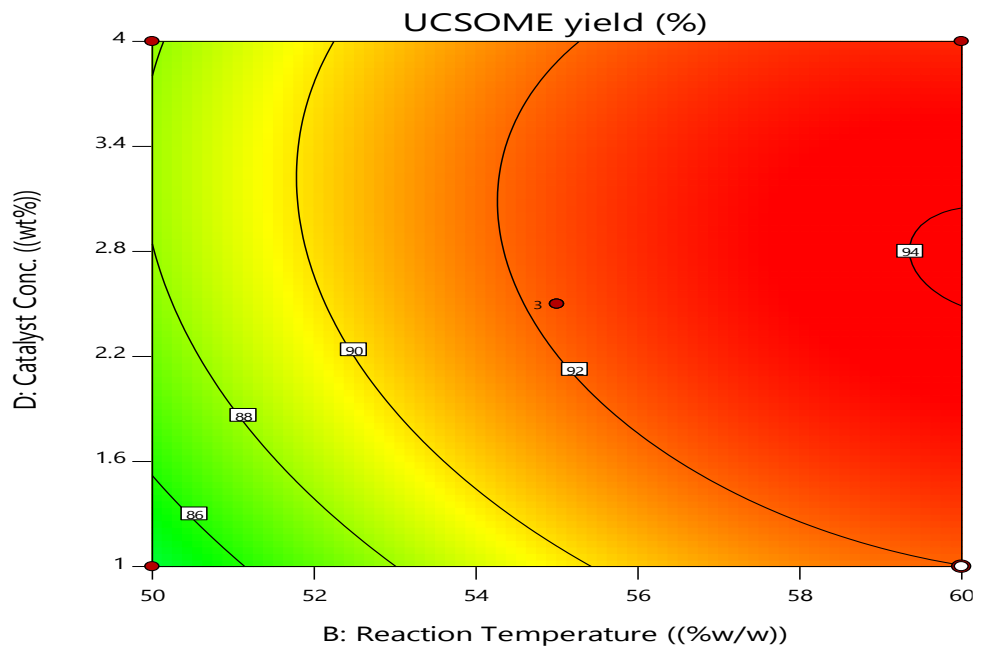


Figure 5b: Contour surface plot between catalyst concentration and reaction temperature at methanol/oil ratio 10.4 and 80min reaction time

Design-Expert® Software

Factor Coding: Actual

UCSOME yield (%)

- Design points above predicted value
- Design points below predicted value

77.4  93.6

X1 = C: Reaction Time

X2 = D: Catalyst Conc.

Actual Factors

A: Methanol/Oil ratio = 10.4

B: Reaction Temperature = 55

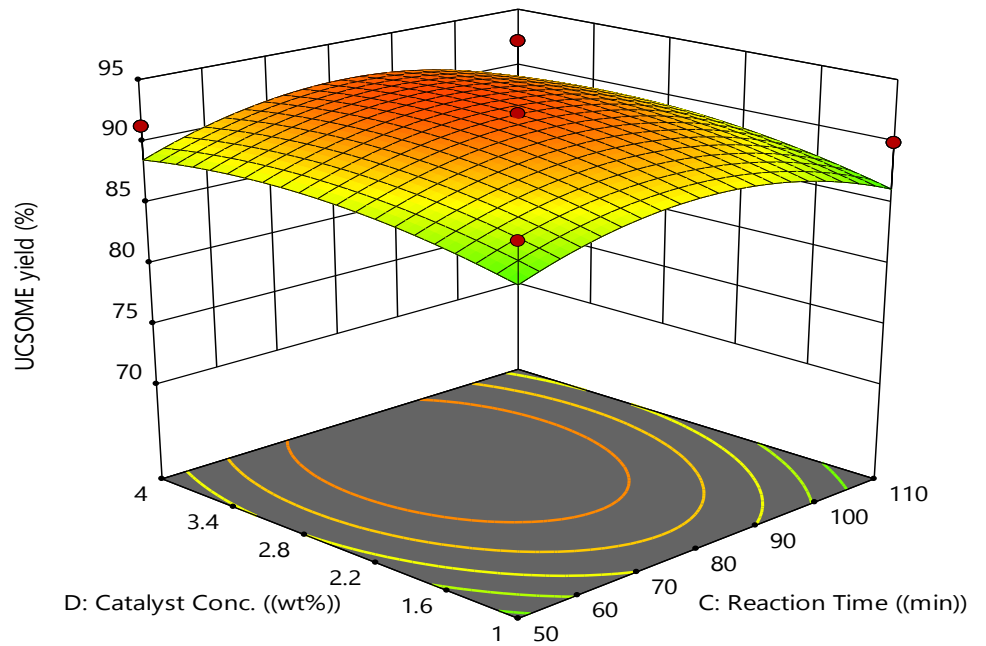


Figure 6a: Response surface plot between catalyst concentration and reaction time at methanol/oil ratio 10.4 and 55 °C reaction temperature

Design-Expert® Software

Factor Coding: Actual

UCSOME yield (%)

● Design Points

77.4  93.6

X1 = C: Reaction Time

X2 = D: Catalyst Conc.

Actual Factors

A: Methanol/Oil ratio = 10.4

B: Reaction Temperature = 55

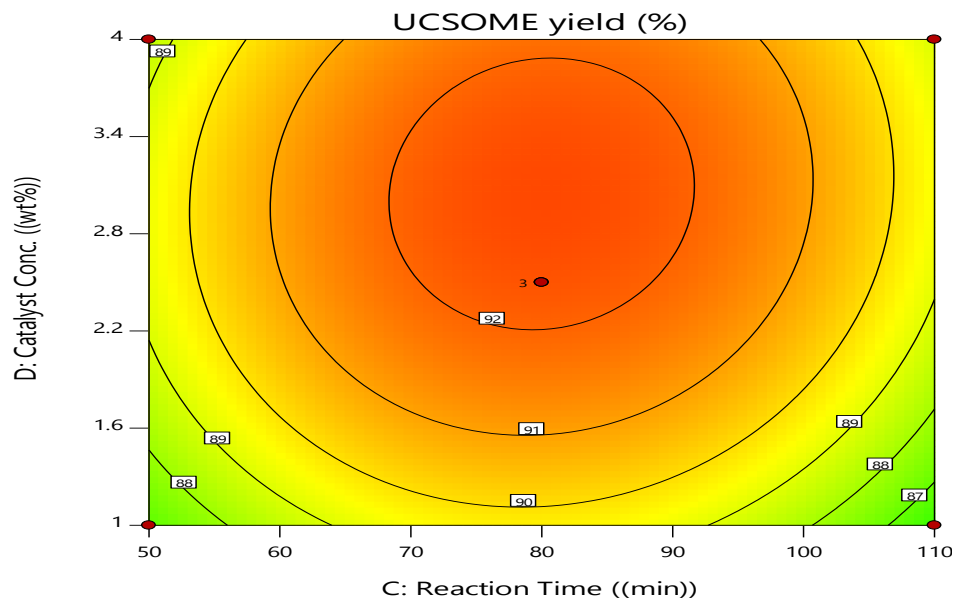


Figure 6b: Contour surface plot between catalyst concentration and reaction time at methanol/oil ratio 10.4 and 55 °C reaction temperature

By producing an overlay plot, the optimization procedure was used to determine the values of the

impacted variables that would produce the best biodiesel yield while taking into consideration all input parameters.

The derived model equation was used to compute the data on the overlay plot in order to identify an optimal location for each variable. Using Design Expert software 11.0.0, the restrictions stated in Table 4 were defined to produce the optimal region:

- (1) The molar ratio was established to be between 10:1 and 10.8:1. However, due to the reaction reversibility, too much methanol is required to move the reaction to the product side.
- (2) The reaction temperature was designed to be between 50 and 60 °C. This is due to methanol boiling point.

Methanol will evaporate if the temperature range is increased above what is necessary for this experiment.

(3) Reaction time is a key element in industry. The goal was to produce as much biodiesel as possible in a short amount of time. Therefore, for the optimization, a reaction time range of 50 to 110 minutes was chosen. The process was optimized based on the established boundaries.

(4) To prevent side reactions with the reactants that could result in soap production, the catalyst concentration goal was chosen at 3.0 wt. %. The process was optimized based on the established boundaries.

Table 4: Numerical Optimization Results and Constraints for the Factors/Response

Parameter	Goal	Experimental Region	
		Lower	Upper
Molar ratio (mol/mol)	In range	10:1	10.8
Reaction temperature (°C)	In range	50	60
Reaction time (min)	In range	50	110
Catalyst concentration (wt. %)	Target	-	3.0
UCSOME YIELD (%)	maximize		

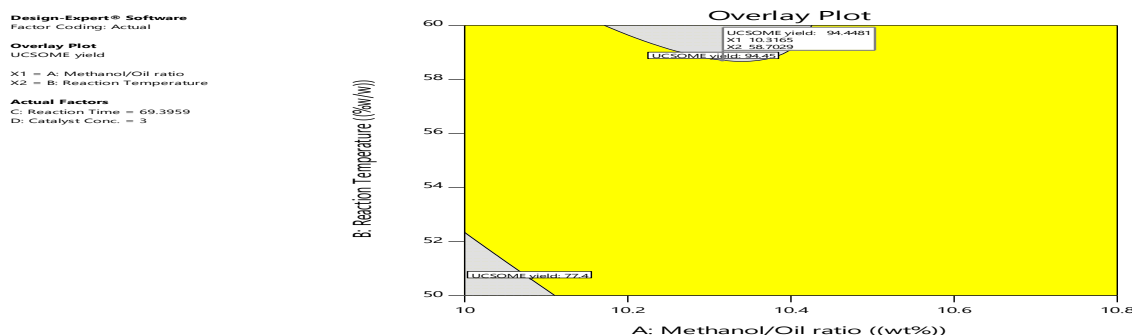


Figure 7: Overlay plot for the prediction of biodiesel production using calcined-hydrated-dehydrated CaO blend heterogeneous catalyst

Within the stated range of input parameters, the plot in Figure 7 shows the response optimal value. The recommended optimum ester yield was 10.32:1 molar alcohol to oil, 3.0 wt.% catalyst concentration, and 94.45 % in 69.39 minutes.

Table 5 for the Box Behnken Design tabulates the results for the independent variables optimum values with the highest yield. The overlay plot was used to determine these values.

Table 5: The Result of Optimum Values

Parameter	Units	Code	BBD Theoretical value
UCSOME YIELD	(%)	Y	94.50
Molar ratio	(mol/mol)	A	10.32:1
Reaction temperature	(°C)	B	58.70
Reaction time	(min)	C	69.39

Catalyst concentration	(g/L)	D	3.0
------------------------	-------	---	-----

Verification of the Design Models

A verification experiment was run in these optimum synthesis conditions to test the correctness of the predicted model. The conducted tests were repeated three times, and the average yield is then tabulated in the model predictions. Table 6 along with

Table 6: Verification of the Design Models

Parameter	Units	Code	BBD Theor. value	Exp. Value
UCSOME YIELD	(%)	Y	94.50	93.70
Molar ratio	(mol/mol)	A	10.30:1	10.30:1
Reaction temperature	(°C)	B	59	59
Reaction time	(min)	C	69.39	69.39
Catalyst concentration	(wt%)	D	3.0	3.0

The average observed value of 93.70 % was comparable to the predicted conversion value of 94.50 %. As a result, there was a respectable level of agreement between the experimentally obtained value and the predicted values. The regression model was successful, as evidenced by the error values between the predicted and observed results

being less than 1% UCSOME conversion. The R-squared in Table 7 was examined in order to confirm the appropriateness of the model. A high R^2 value is preferred, and it is critical that adjusted R^2 and predicted R^2 coincide to a reasonable degree [63]. The difference between adjusted R^2 and predicted R^2 was less than 0.2.

Table 7: The R-Squared Results

Std. Dev.	1.19	R^2	0.9953
Mean	74.38	Adjusted R^2	0.9898
C.V. %	1.61	Predicted R^2	0.975
PRESS	90.64	Adeq	40.6226
		Precision	
-2 Log Likelihood	64.34	BIC	113.77
		AICc	137.97

As a measure of the experimental signal-to-noise ratio, adequate precision (AP) [64]; an AP that exceeds 4 usually indicates that the model will give a reasonable performance in prediction. The "Adeq Precision" for this study was 40.6226. As a result, the model might be utilized to explore the design space. A crucial phase in

the model structure sequence is model validation. The validation of a model frequently looks to be as simple as stating the R^2 fit values (which measures the fraction of the total variability in the response that is accounted for by the model).

Design-Expert® Software

UCSOME yield

Color points by value of UCSOME yield:

77.4 93.6

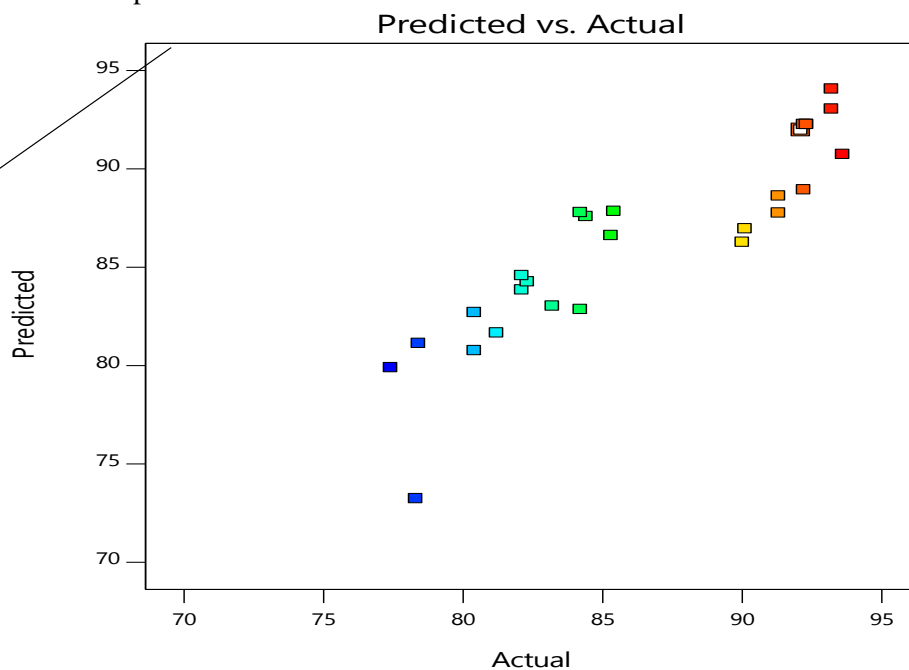


Figure 8: The biodiesel conversion predicted from model versus measured response

The Predicted by Actual plot offers a graphical evaluation of model fit that considers variation brought on by random events. It compares the actual values to the forecasted values on a graph. Figure 8 shows a plot of the

actual values and predicted values for the conversion of UCSO to UCSOME using a heterogeneous catalyst CaO blend. The values were rather close to the 45-degree line, which shows a good

experimental error using a normal plot of residuals. Following the estimation of all the unknown model parameters from the experimental data, the predicted response is determined using the selected model. Examining residuals is an essential component of all statistical modeling since it offers helpful information about how well the model fits the data, as seen in figure 9.

correlation between the predictions and the actual outcomes of the model. By deducting the actual responses from the predicted responses, one can estimate the

Design-Expert® Software

UCSOME yield

Color points by value of UCSOME yield:

77.4  93.6

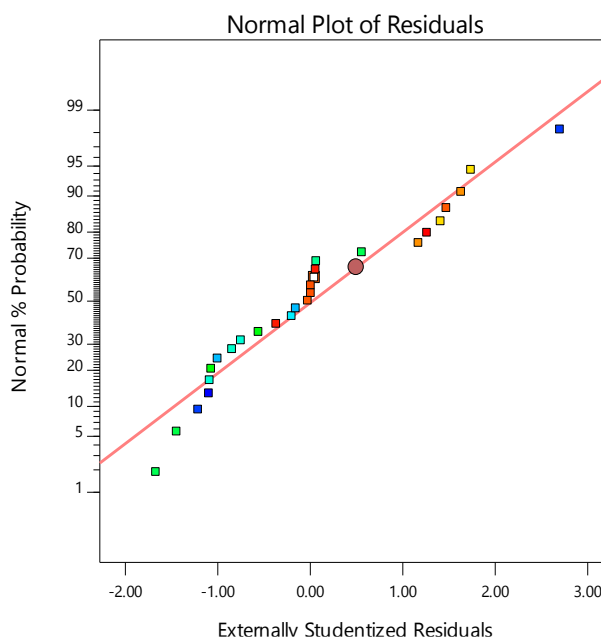


Figure 9: Normal plot of residuals


Generally speaking, the residuals should have a random distribution, be devoid of evident patterns, and have unexpected values. Because the pattern closely resembles a straight line and there are no outliers, the normal plot

(Fig. 9) shows that the data set utilized for this experiment is normally distributed. This suggests that the model corresponds to the experimental data

Design-Expert® Software

UCSOME yield

Color points by value of UCSOME yield:

77.4  93.6

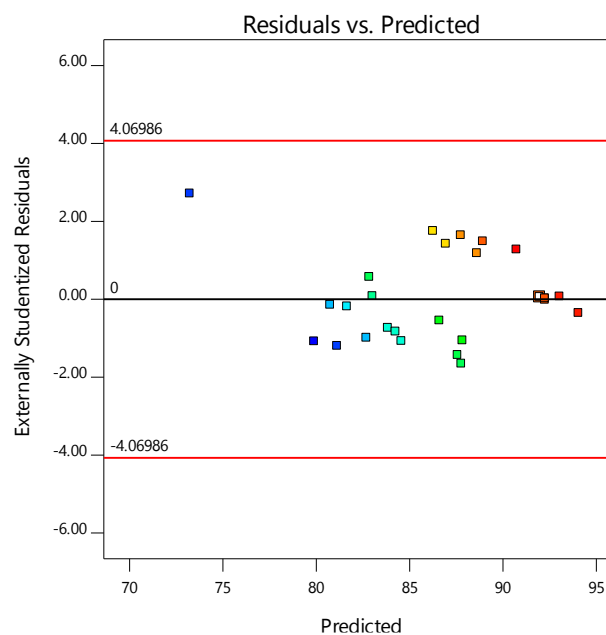


Figure 10: Residuals vs predicted values

Design-Expert® Software

UCSOME yield

Color points by value of UCSOME yield:

77.4  93.6

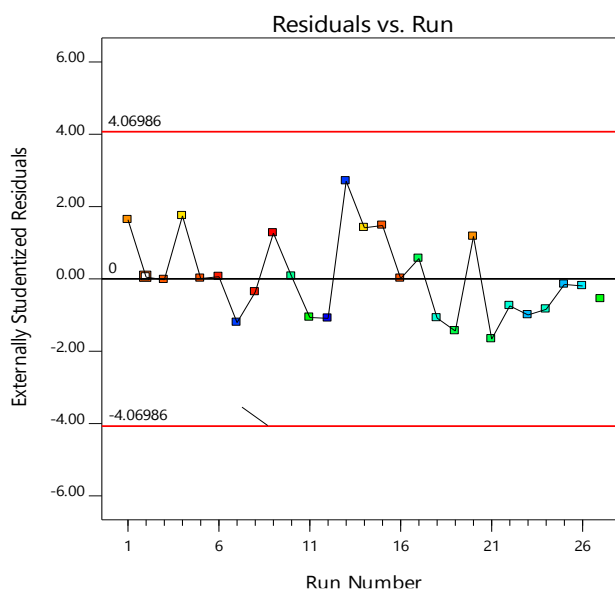


Figure 11: Residuals vs run a number

The fact that the data points in Figure 10 are dispersed randomly without establishing a pattern supports the presumption that the residuals are constant. The residuals versus run plot are used to confirm the notion that the residuals are unrelated to one another.

The points in figure 11 are distributed randomly around the centerline, proving the independence of the residual. Independent residuals do not exhibit any trends or patterns when displayed in run order

Table 8: Results of the current study compared with other related investigations

Optimum parameters	Feedstock	%Yield	References
Calcined-hydrated-dehydrated CaO- blend (from eggshell & coconut husk waste) 2.5 wt%, 10:1, 60 °C, 80 min	Used cottonseed oil(UCSO)	93.60	This paper
Calcined-hydrated-dehydrated CaO (from eggshell) 5.0 wt%, 12:1, 65°C, 60 min	Waste frying oil(WFO)	94.52	[39]
KOH 1 wt%, 7:1, 40°C, 800 rpm	Shea biodiesel	92.16	[65]
NaOH 1.1 wt%, 7:1, 60°C, 600 rpm, 15 min	Used frying oil	88.80	[66]
Enzyme load (2 g), 12:1, 35°C,	Waste cooking oil	93.61	[67]
Silica sulfuric acid 5 %, 20:1, 373 K 8 hr	Cottonseed oil	97.86	[68]
CaO/KOH 7 wt%, 12:1, 65 °C, 120 min	Waste cooking oil	87.17	[69]
CaO (from waste eggshell & rice husk) 1 wt%, 20:1, 60°C, 120 min	Waste cooking oil	87.50	[70]

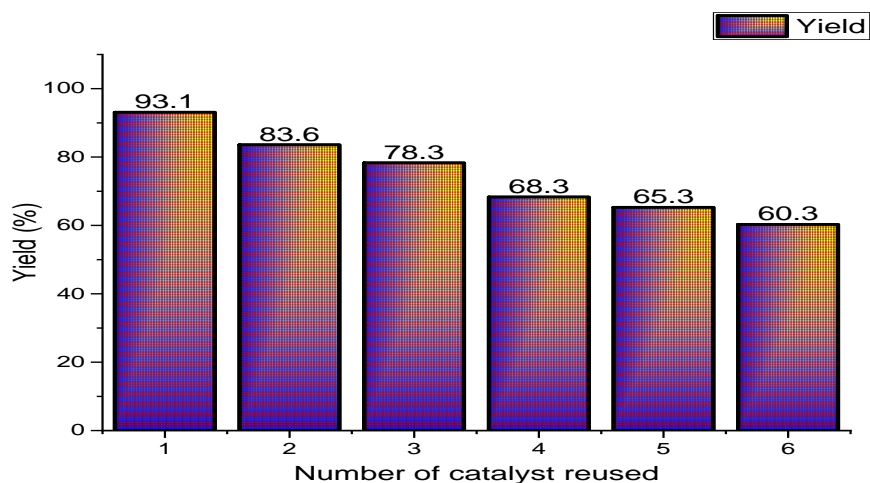


Figure 12: Effect of Reusability of Catalyst on FAME Yield

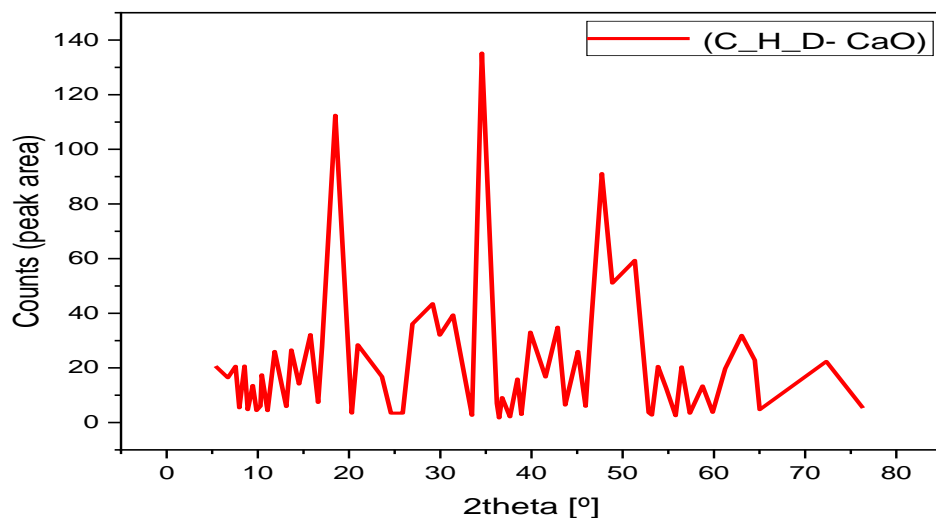


Figure 13: XRD Analysis of calcined-hydrated-dehydrated CaO (C_H_D- CaO)

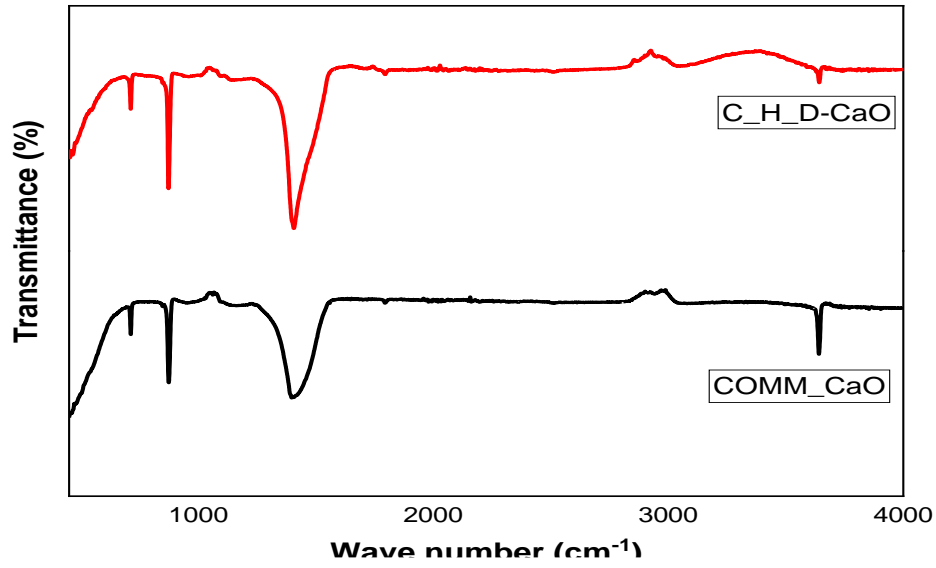


Figure 14: FTIR spectra of the commercial (COMM_CaO) and calcined-hydrated-dehydrated CaO (C_H_D- CaO)

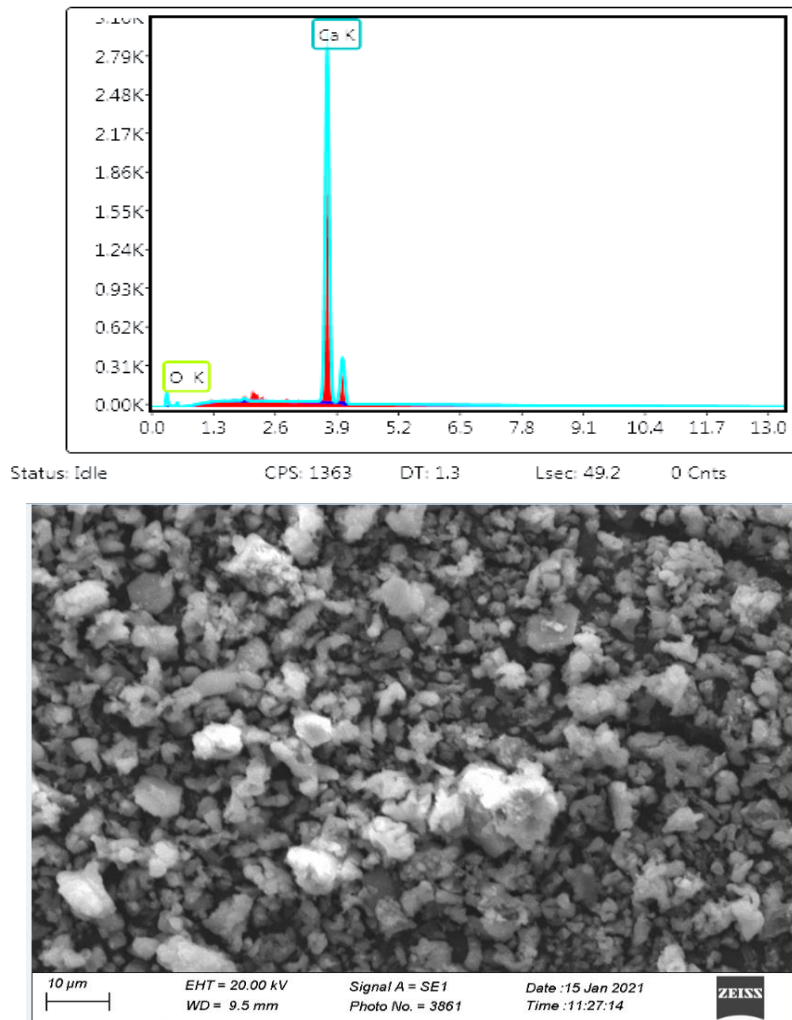


Figure 15: Micrograph and EDX of calcined-hydrated-dehydrated CaO (C_H_D- CaO)

FTIR Analysis of Used Cotton Seed Oil (UCSO) and Used Cotton Seed Oil Methyl Ester (UCSOME)

Used Cotton Seed Oil and Used Cotton Seed Oil Methyl Ester exhibit high absorption at 2992 cm^{-1} in their respective IR spectra (Tables 9 and 10; Figures 16 and 17), which is caused by the aliphatic CH_2 symmetric stretching vibration of the group. The large percentage of the linoleic acid group (33.43 %) could be the cause of this (Table 11a & Table 12a). Similar findings were made with yellow oleander seed oil [71]. They exhibit absorbance at the following other distances: 1744 cm^{-1} , 1461 cm^{-1} , 1375 cm^{-1} , 1159 cm^{-1} , 964 cm^{-1} , and 723 cm^{-1} . However, there is a distinction between the spectra of the oils. Significant variations that are caused by the production of biodiesels can be shown in a comparative analysis of the FTIR peaks of the functional groups of the oils and their respective biodiesel. Biodiesel fatty acid methyl ester possesses a distinctive FTIR absorption of

carbonyl ($\text{C}=\text{O}$) stretching vibrations near $1740\text{-}1744\text{ cm}^{-1}$ and C-O bending vibrations in the range of 1196 cm^{-1} . The characterization and quantification of FAMES in biodiesel and used cotton seed oil by IR spectroscopy is based on this spectrum separation between the functional groups of used vegetable oils and their corresponding biodiesel [71]. The production of a signal at 1438 cm^{-1} (fig.13), which corresponds to the deformation vibration of the methyl ester group (CO)- O-CH_3 present in the biodiesel spectrum which is lacking in the oil spectrum, served as a signal for the influence of transesterification. A similar result was reported by [72]. Another visible transformation revealed by the FTIR spectra of FAMES is a signal around 1170 cm^{-1} of the C-O group in the ester-controlled area and the appearance of a signal at 964 cm^{-1} corresponding to CH_2 in RCOCO group present in the oil and absent in the FAMES.

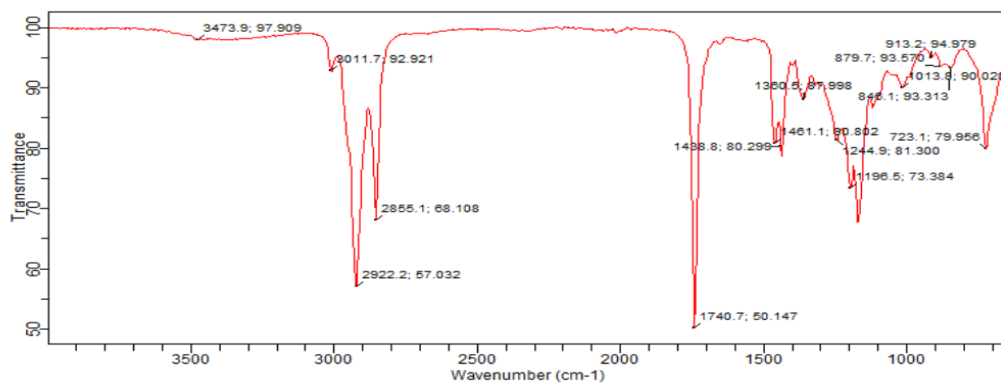


Figure 16: FTIR spectra of Used Cotton Seed Oil Methyl Ester (UCSOME)

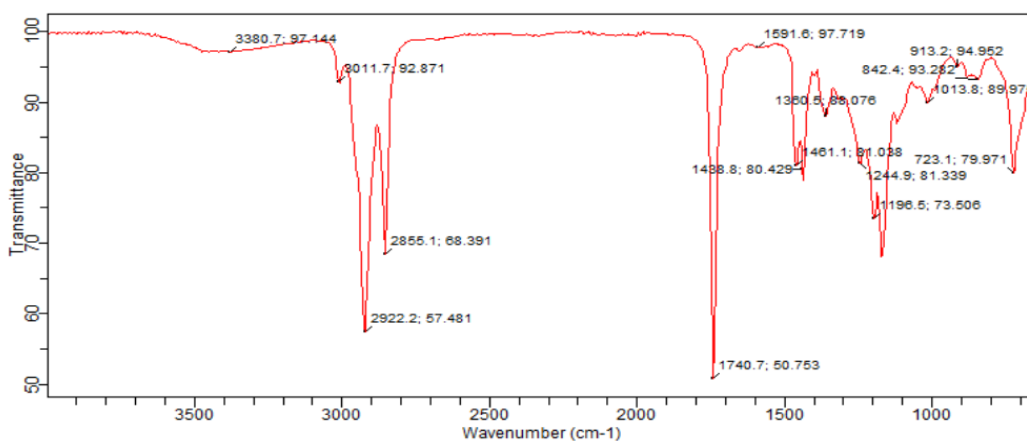


Figure 17: FTIR spectrum of Used Cottonseed Oil (UCSO)

Table 9: Interpretation of FTIR peaks (cm⁻¹) in Used Cotton Seed Oil (UCSO)

SN	Peaks (cm ⁻¹)	Transmittance (%)	Remarks
1	2922.2	57.481	Symmetric and asymmetric stretching vibrations of the aliphatic -CH ₂ and -CH ₃ groups
2	2855.1	68.391	Symmetric and asymmetric stretching vibrations of the aliphatic -CH ₂ and -CH ₃ groups.
3	1740.7	50.753	Double bond stretching -ester carbonyl functional group of the triglycerides
4	1461.1	81.038	Long linear aliphatic chain of bounded and free fatty acids attached to triglyceride.
5	1380.5	88.078	O-CH ₂ present in triglyceride
6	1249.5	81.339	C-H/C-N presence.
7	1196.5	73.506	Fingerprint region -C-O stretching vibration of an ester group
8	723.1	79.971	Overlapping of the CH ₂ rocking vibration and the out-of-plane vibration of disubstituted olefins.

Table 10: Interpretation of FTIR peaks (cm⁻¹) in Used Cotton Seed Oil Methyl Ester (UCSOME)

1	Peaks (cm ⁻¹)	Transmittance (%)	Remark
1	2922.2	57.032	Symmetric and asymmetric stretching vibrations of the aliphatic -CH ₂ and -CH ₃ groups
2	2855.1	68.108	Symmetric and asymmetric stretching vibrations of the aliphatic -CH ₂ and -CH ₃ groups.
3	1740.7	60.147	Double bond stretching-ester carbonyl functional group of the triglycerides
4	1488.8	80.299	Long linear aliphatic chain of bounded and free fatty acids attached to triglyceride.
5	1461.1	80.802	(CO) – O – CH ₃ of methyl ester present
6	1380.5	87.998	O-CH ₂ present in triglyceride
7	1244.9	81.300	C-H/C-N presence.
8	1196.5	73.384	Fingerprint region-C-O stretching vibration of ester group in biodiesel
9	1013.8	90.028	The C - O stretching of – O-CH ₂ –C
10	723.1	79.956	Overlapping of the CH ₂ rocking vibration and the out-of-plane vibration of disubstituted olefins.

GC-MS Analysis

Fatty Acid Compositions of Used Cotton Seed Oil (UCSO) and Used Cotton Seed Oil Methyl Ester (UCSOME). The composition of fatty acids in UCSO is depicted in a gas chromatogram (figure 18), and their respective primary peaks and percentage compositions as listed in Tables 11a and b. Palmitic acid, linoleic acid, 11-Octadecenoic acid, Linoelaidic acid, stearic acid, and Lauric acid are the main fatty acids. With Lauric acid at 1.78 %, stearic acid at 2.42 %, Linoelaidic acid at 7.69 %, 11-Octadecenoic acid at 16.04 %, linoleic acid at 25.65 %, and palmitic acid at 33.57 %, the profile proves a high percentage of saturated and unsaturated fatty acids. UCSO shows a higher percentage of unsaturated than the saturated fatty acids with stearic and palmitic acid which are the saturated fatty acids, and linoleic acid which is the unsaturated fatty acid. Due to the methylation of the oil before the GC-MS study, almost all of the free fatty acids were in their methyl ester derivatives. The molecular ions of the methyl derivatives are 14 mass units higher than those of the parent compounds, but they have the same

fragmentation patterns [73]. Thirty-four (34) different chemicals, including methyl esters, butyl esters, steroids, dihydric alcohols, naphthalene, and phenolic compounds, are found in the UCSO according to the GC-MS study. The therapeutic benefits of UCSO are due to the large variety of substances present in it, including phytochemicals like Phytosterols, Tocopherols, Carotenoids, and Polyphenols. [74] insist that these phytochemicals can be used to make pharmaceuticals, cosmetics, and food since they have strong antibacterial, antioxidant, antiproliferation, and anticancer effects. The GC-MS result shows the different concentrations of methyl esters of saturated and unsaturated fatty acids. However, palmitic acid still leads with its relative percentage of 33.57%, followed by linoleic acid with 25.65% and 11-Octadecenoic acid with 16.04%. The saturation of Palmitic and Stearic acid could be the result of relative oxidative and thermal stability possessed by UCSO, although polyunsaturated fatty acid methyl esters are prone to auto-oxidation UCSO is more stable relative to other polyunsaturated oils such as mustard (94.27%) and sunflower (88.39%) [75]. The need for linoleic acid

in the cosmetics sector is rising [76]. When extracted, palmitic acid has a high economic value, and because it is unsaturated, it has been suggested that it can enhance the flow characteristics. Furthermore, soap, cosmetics, and releasing agents are made with the sodium salt of palmitic acid [77]. According to reports, highly saturated oils have greater cloud points and cetane numbers and are more stable [78]. Chain length and the amount of vacant bonds are two factors that affect several aspects of biodiesel [79]. Similar to this, Figure 19 Gas Chromatogram depicts the composition of fatty acids in UCSOME, whereas Tables 12a & b shows respective significant peaks and % compositions. The main fatty acids found in the methyl esters include palmitic acid, linoleic acid, lauric acid, myristic acid, stearic acid, and arachidic acid. The profile shows a high percentage of saturated fatty acids with palmitic acid at 29.64%, Lauric acid at 8.10%, Myristic acid at 6.67%, Stearic acid at 5.60%, Arachidic acid at 1.17%, and linoleic acid as 33.43%. UCSOME shows a higher percentage of saturated than the unsaturated fatty acids with linoleic acid at 33.43% exhibiting the major peak for the unsaturated fatty acid of the ester. The major fatty esters in UCSOME are Lauric acid (C12:0), Linoleic ester (19:2), Palmitic ester (C16:0), Stearic ester (C18:0), and Myristic acid (C14:0). Also, the nature of fatty acids plays a significant role in the properties of biodiesel (Table 12b). The fatty acid content resembles that which

was described by [80]. The high percentage of the polyunsaturated fatty acid in UCSOME fuel increases its risk of undergoing auto-oxidation and rancidity, thereby affecting its storage property. High cloud points and other fuel properties discovered in this investigation were also indicative of the increased proportion of polyunsaturated fatty acids in UCSOME. The high heat of combustion of 38.905 MJ/kg of palmitic acid, a saturated fatty acid, contributed significantly to the energy value of UCSOME. A good indication that UCSOME can replace fossil fuel is its high fatty acid content (92.00 %) [81][82][83]. These findings closely align with earlier reports on the FA profile of CSO [84]. The transesterification of saturated and monounsaturated fatty acids produces the majority of the biodiesel, with the remainder polyunsaturated and some bulk saturated fatty acids contributing to its high viscosity. Because they are easily oxidized, unsaturated fatty acids with a larger concentration degrade the quality of fuel. Generally speaking, unsaturated fatty acids like 18:1, 18:2, and 18:3 are less stable than saturated ones like 16:0 or 18:0, which lowers the fuel property. The result also demonstrates that transesterification-produced biodiesel methyl esters have higher percentages of saturated fatty acids and lower percentages of unsaturated fatty acids. The produced biodiesel has higher viscosity, a higher cetane number, and improved biodiesel stability due to the inclusion of saturated fatty acids.

Table 11a: Fatty acid Composition of the UCSO and their Relative Percentages

Common Name	Symbol	Percentage of the total weight
Capric acid methyl ester	C11:0	0.23
Caprylic acid methyl ester	C09:0	1.05
Azelaaldehydic acid, methyl ester	C10:0	0.99
Myristic acid	C15:0	1.63
Lauric acid, methyl ester	C13:0	1.78
Methyl palmitoleate	C17:1	0.82
Palmitic acid, methyl ester	C17:0	33.57
Methyl 8-heptadecenoate	C18:1	0.17
Margaric acid methyl ester	C18:0	0.11
Linoleic acid, methyl ester	C19:2	25.65
11-Octadecenoic acid, methyl ester	C19:1	16.04
Methyl stearate	C19:0	2.42
Cyclopropaneoctanoic acid, 2-octyl, methyl ester	C20:0	0.35
7,10-Octadecadienoic acid, methyl ester	C19:2	0.15
Linolenic acid, methyl ester	C19:3	0.2
6,9-Octadecadienoic acid, methyl ester	C19:2	0.15
Linolelaidic acid, methyl ester	C19:2	0.70
Methyl 12-hydroxy-9-octadecenoate	C19:1	0.39
Arachidic acid methyl ester	C21:0	0.38
Behenic acid, methyl ester	C23:0	0.05
Linoelaidic acid	C19:4	7.69
Others		5.48

Table 11b: Major Resolved Peak areas of Used Cotton Seed Oil (UCSO) Gas Chromatogram and their Suggested Compound from NIST14 library

Peak No	Retention Time (min)	Area (%)	Compounds
6	22.78	1.78	Lauric acid, methyl ester
7	27.55	1.63	Myristic acid
10	30.70	33.57	Palmitic acid, methyl ester
11	31.11	2.32	n-Hexadecanoic acid
16	32.14	25.51	9,12-Octadecadienoic acid (Z,Z)-, methyl ester
17	32.18	16.04	11-Octadecenoic acid, methyl ester
18	32.31	2.42	Methyl stearate
19	32.49	7.69	Linoelaidic acid

Table 12a: Fatty acid Composition of the UCSOME and their Relative Percentages

Common Name	Symbol	Percentage of the total weight
Myristic acid	C14:0	6.67
Linoleic acid, methyl ester	C19:2	33.43
Palmitic acid	C16:0	29.64
Lauric acid	C12:0	8.10
Caprylic acid methyl ester	C9:0	1.05
Methyl stearate	C19:0	5.60
Arachidic acid	C20:0	1.17
Capric acid methyl ester	C11:0	0.88
cis-10-Heptadecenoic acid, methyl ester	C18:1	0.73
Methyl 2-octylcyclopropene-1-octanoate	C12:1	0.64
Linoleic acid ethyl ester	C20:2	0.36
Docosanoic acid, methyl ester	C23:0	0.29
Pentadecanoic acid, methyl ester	C16:0	0.18
Methyl eladate	C19:1	0.15
Hexadecanoic acid, 14-methyl-, methyl ester	C18:0	0.26
Nonanoic acid, 9-oxo-, methyl ester	C10:0	0.14
Heneicosanoic acid, methyl ester	C22:0	0.12
Others		3.68

Table 12b: Major resolved peak areas of Used Cotton Seed Oil Methyl Ester (UCSOME) Gas Chromatogram and their Suggested Compound from NIST14 library

Peak No	Retention Time (min)	Area (%)	Compounds
25	28.04	6.67	Myristic acid
27	30.89	29.64	Arachidic acid
32	32.31	33.43	Linoleic acid, methyl ester
33	32.99	5.60	Methyl stearate
36	33.75	1.17	Arachidic acid

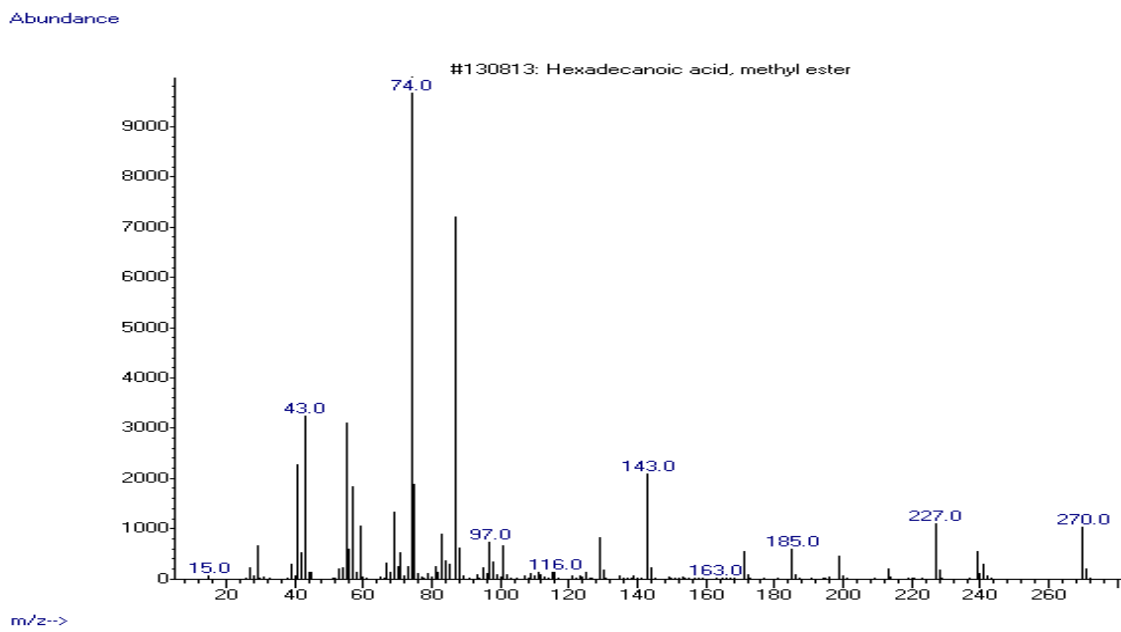
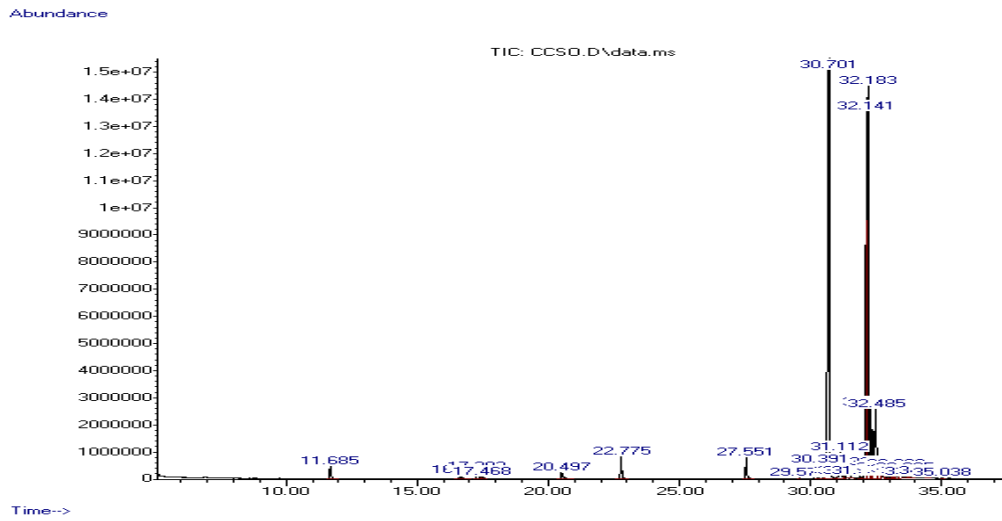
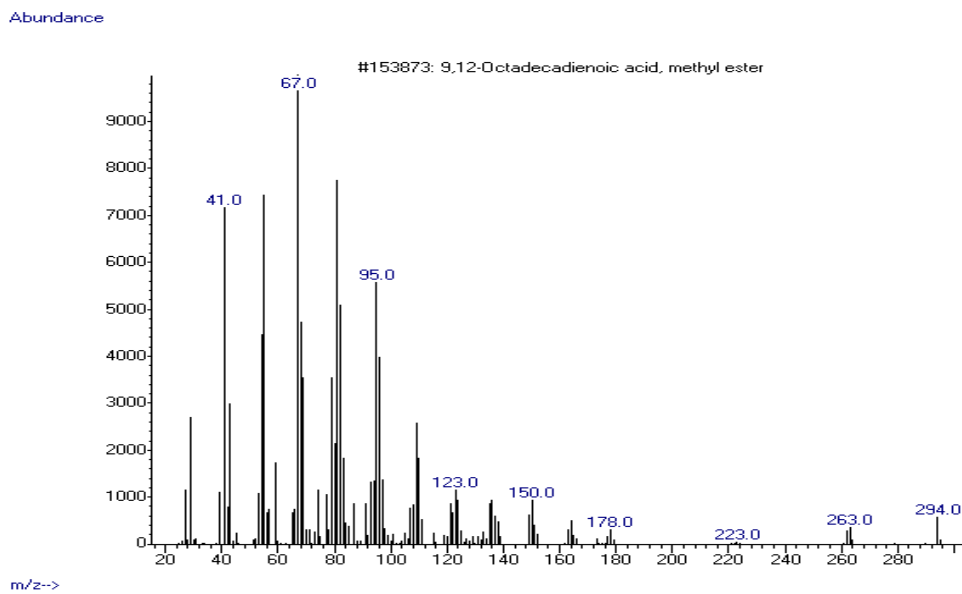


Figure 18: Gas chromatogram of some Used Cotton Seed Oil (UCSO)



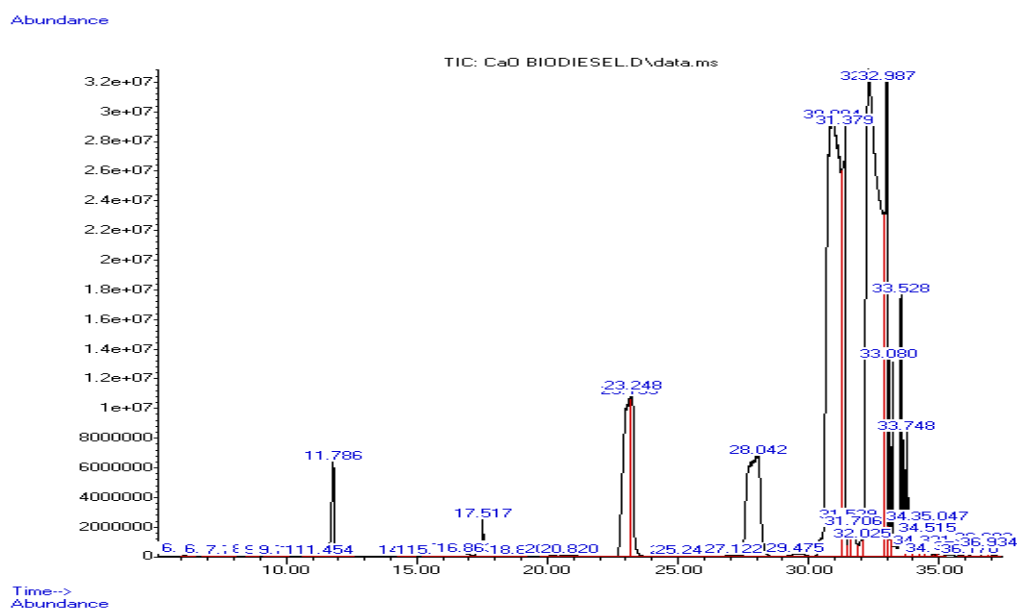


Figure 19: Gas chromatogram of Used Cotton Seed Oil Methyl Ester (UCSOME)

Conclusion

The current study examines how several process variables, including the molar ratio, catalyst concentration, reaction temperature, and reaction time, affect the yield of UCSOME. Based on its FFA value, the one-time UCSO was utilized to analyze the effects of reaction parameters on the biodiesel production process. Alkaline transesterification is a reliable technique for producing biodiesel, as evidenced by the 1.26 % FFA value of UCSO. The goal of the research in this study was to improve the independent reaction components in order to maximize the yield of biodiesel using a mathematical equation using RSM. At a 10-molar ratio, 2.5 wt. % catalyst loading, 80 min of reaction time, and 60 °C reaction temperature, the highest biodiesel yield of 93.60 % was achieved. The experimental trial was conducted using the optimized condition, and it was discovered that the experimental yield of 93.70 % and the predicted yield

of 94.50 % have a strong correlation. The smallest percent inaccuracy, 0.84 %, was discovered to exist. RSM has therefore been verified to be a successful approach in predicting the key variables that influence the biodiesel production yield. The fatty acid methyl esters of UCSO showed pronounced carbonyl (C=O) stretching vibrations in the region of 1740.7 cm^{-1} in their FTIR spectra. The appearance of a signal at 1461.1 cm^{-1} for the (CO)-O-CH₃ group (a methyl ester group) in the biodiesel spectra indicated the result of the transesterification. Because of the C=O functional groups in fossil diesel, there are no such absorptions. Similarly, the GC-MS result indicated that UCSOME had around 95% saturated/unsaturated fatty esters, indicating the potential for high heats of combustion a suitable replacement for fossil diesel. Further proving the synthesized CaO as a renewable catalyst was the characterization of the catalyst using XRD and SEM analyses.

Acknowledgments

The management of the Multi-User Scientific Research Laboratory at Ahmadu Bello University in Zaria is gratefully acknowledged by the authors for providing the laboratory space necessary for this investigation.

Declarations

Funding: This work was funded by the management of Petroleum Technology Development Fund (PTDF), under PTDF Local Scholarship Scheme (LSS-PhD) number PTDF/ED/LSS/PHD/JA/0329/19; (19PHD0108).

Conflicts of interest: The authors declare no conflict of interest

Availability of data and material: Not applicable

Code availability: Not applicable

Ethics approval: Not applicable

Consent to participate: Not applicable

Consent for publication: Not applicable

Credit Author Statement

Abdullateef Jimoh: Conceptualization, Investigation, funding acquisition, Formal analysis, writing original, draft, Resources.

Sani Uba: Conceptualization, supervision, project administration, writing review and editing, Resources.

Victor .O. Ajibola: Conceptualization, supervision, project administration, writing review and editing, Resources.

Edith .B. Agbaji: Conceptualization, supervision, writing review and editing, Resources.

Reference

[1] N. Jeyakumar, B. Narayanasamy, V. Balasubramaniam, Optimization of used cooking oil methyl ester production using

- response surface methodology. *Energy Sources, Part A: Recovery, Utilization, and Environmental Effects*, 41 (2019) 2313-2325.
- [2] A. Berwal, A. Dahiya, P. Berwal, Production of Biodiesel from Karanja oil. *Journal of Alternate Energy Sources and Technologies*, 5 (2014) 43-49.
- [3] G. Tüccar, E. Uludamar, Emission and engine performance analysis of a diesel engine using hydrogen enriched pomegranate seed oil biodiesel. *Int. J. Hydrogen Energy*, 43 (2018) 18014-18019.
- [4] S.A. Razack, S. Durairasan, Response surface methodology assisted biodiesel production from waste cooking oil using encapsulated mixed enzyme. *Waste Management*, 47 (2016) 98-104.
- [5] M. Cetinkaya, F. Karaosmanoğlu, Optimization of base-catalyzed transesterification reaction of used cooking oil. *Energy & fuels*, 18 (2004) 1888-1895.
- [6] K.-C. Ho, C.-L. Chen, P.-X. Hsiao, M.-S. Wu, C.-C. Huang, J.-S. Chang, Biodiesel production from waste cooking oil by two-step catalytic conversion. *Energy Procedia*, 61 (2014) 1302-1305.
- [7] K. Colombo, L. Ender, A.A.C. Barros, The study of biodiesel production using CaO as a heterogeneous catalytic reaction. *Egyptian Journal of Petroleum*, 26 (2017) 341-349.
- [8] P. Felizardo, M.J.N. Correia, I. Raposo, J.F. Mendes, R. Berkemeier, J.M. Bordado, Production of biodiesel from waste frying oils. *Waste management*, 26 (2006) 487-494.
- [9] S. Nagesh, T. Chandrashekhar, N. Banapurmath, Injection timing effect on the performance of diesel engine fueled with acid oil methyl ester, IOP Conference Series: Materials Science and Engineering, IOP Publishing, 2018, pp. 012002.
- [10] F.H. Alhassan, U. Rashid, Y.H. Taufiq-Yap, Optimization of simultaneous production of waste cooking oil based-biodiesel using iron-manganese doped zirconia-supported molybdenum oxide nanoparticles catalyst. *Journal of Renewable and Sustainable Energy*, 8 (2016) 033101.
- [11] J. Milano, H.C. Ong, H.H. Masjuki, A.S. Silitonga, W.-H. Chen, F. Kusumo, S. Dharma, A.H. Sebayang, Optimization of biodiesel production by microwave irradiation-assisted transesterification for waste cooking oil-Calophyllum inophyllum oil via response surface methodology. *Energy conversion and management*, 158 (2018) 400-415.
- [12] S. Karimifard, M.R.A. Moghaddam, Application of response surface methodology in physicochemical removal of dyes from wastewater: a critical review. *Science of the Total Environment*, 640 (2018) 772-797.
- [13] S. Semwal, A.K. Arora, R.P. Badoni, D.K. Tuli, Biodiesel production using heterogeneous catalysts. *Bioresource technology*, 102 (2011) 2151-2161.
- [14] Y. Feng, A. Zhang, J. Li, B. He, A continuous process for biodiesel production in a fixed bed reactor packed with cation-exchange resin as heterogeneous catalyst. *Bioresource Technology*, 102 (2011) 3607-3609.
- [15] N. Zhang, H. Xue, R. Hu, The activity and stability of CeO₂@ CaO catalysts for the production of biodiesel. *RSC Adv.*, 8 (2018) 32922-32929.
- [16] M.E. Borges, L. Díaz, Recent developments on heterogeneous catalysts for biodiesel production by oil esterification and transesterification reactions: A review. *Renewable and Sustainable Energy Reviews*, 16 (2012) 2839-2849.
- [17] X. Liu, H. He, Y. Wang, S. Zhu, X. Piao, Transesterification of soybean oil to biodiesel using CaO as a solid base catalyst. *Fuel*, 87 (2008) 216-221.
- [18] E. Viola, A. Blasi, V. Valerio, I. Guidi, F. Zimbardi, G. Braccio, G. Giordano, Biodiesel from fried vegetable oils via transesterification by heterogeneous catalysis. *Catalysis Today*, 179 (2012) 185-190.
- [19] Z. Huaping, W. Zongbin, C. Yuanxiong, P. Zhang, D. Shijie, L. Xiaohua, M. Zongqiang, Preparation of biodiesel catalyzed by solid super base of calcium oxide and its refining process. *Chinese Journal of Catalysis*, 27 (2006) 391-396.
- [20] K. Shah, K. Maheria, J. Parikh, Effect of reaction parameters on the catalytic transesterification of cottonseed oil using silica sulfuric acid. *Energy Sources, Part A: Recovery, Utilization, and Environmental Effects*, 38 (2016) 1470-1477.
- [21] M.N. Nabi, S.N. Hoque, M.S. Akhter, Karanja (*Pongamia Pinnata*) biodiesel production in Bangladesh, characterization of karanja biodiesel and its effect on diesel emissions. *Fuel processing technology*, 90 (2009) 1080-1086.
- [22] B. Masum, H. Masjuki, M. Kalam, I.R. Fattah, S. Palash, M. Abedin, Effect of ethanol-gasoline blend on NO_x emission in SI engine. *Renewable and Sustainable Energy Reviews*, 24 (2013) 209-222.
- [23] A.K. Agarwal, Biofuels (alcohols and biodiesel) applications as fuels for internal combustion engines. *Progress in energy and combustion science*, 33 (2007) 233-271.
- [24] J. Xue, T.E. Grift, A.C. Hansen, Effect of biodiesel on engine performances and emissions. *Renewable and Sustainable energy reviews*, 15 (2011) 1098-1116.
- [25] D. Qi, H. Chen, L. Geng, Y. Bian, Effect of diethyl ether and ethanol additives on the combustion and emission characteristics of biodiesel-diesel blended fuel engine. *Renewable energy*, 36 (2011) 1252-1258.
- [26] H. Hamze, M. Akia, F. Yazdani, Optimization of biodiesel production from the waste cooking oil using response surface methodology. *Process Safety and Environmental Protection*, 94 (2015) 1-10.
- [27] A.S. Bharadwaj, M. Singh, S. Niju, K.M.S. Begum, N. Anantharaman, Biodiesel production from rubber seed oil using calcium oxide derived from eggshell as catalyst-optimization and modeling studies. *Green Processing and Synthesis*, 8 (2019) 430-442.
- [28] B. Yoosuk, P. Udomsap, B. Puttasawat, P. Krasae, Modification of calcite by hydration-dehydration method for heterogeneous biodiesel production process: The effects of water on properties and activity. *Chemical Engineering Journal*, 162 (2010) 135-141.
- [29] S.C. Sekhar, K. Karuppusamy, N. Vedaraman, A. Kabeel, R. Sathyamurthy, M. Elkelawy, H.A.E. Bastawissi, Biodiesel production process optimization from *Pithecellobium dulce* seed oil: Performance, combustion, and emission analysis on compression ignition engine fuelled with diesel/biodiesel blends. *Energy conversion and management*, 161 (2018) 141-154.
- [30] H.T. Nguyen, C.L. Walker, E.A. Walker, A first course in fuzzy logic, CRC press(2018).
- [31] C. De Blasio, C. De Blasio, Biodiesel. *Fundamentals of Biofuels Engineering and Technology*, (2019) 253-265.
- [32] F.B. Shahri, A. Niazi, Synthesis of modified maghemite nanoparticles and its application for removal of acridine orange from aqueous solutions by using Box-Behnken design. *Journal of Magnetism and Magnetic Materials*, 396 (2015) 318-326.

- [33] M.C. Sekhar, B.P. Reddy, K. Mallikarjuna, G. Shanmugam, C.-H. Ahn, S.-H. Park, Synthesis, characterization, and analysis of enhanced photocatalytic activity of Zr-doped TiO₂ nanostructured powders under UV light. *Materials Research Express*, 5 (2018) 015024.
- [34] G.A. Miraculas, N. Bose, R.E. Raj, Process parameter optimization for biodiesel production from mixed feedstock using empirical model. *Sustainable Energy Technologies and Assessments*, 28 (2018) 54-59.
- [35] R. Foroutan, R. Mohammadi, H. Esmaili, F.M. Bektashi, S. Tamjidi, Transesterification of waste edible oils to biodiesel using calcium oxide@ magnesium oxide nanocatalyst. *Waste Management*, 105 (2020) 373-383.
- [36] Y.H. Tan, M.O. Abdullah, C. Nolasco-Hipolito, Y.H. Taufiq-Yap, Waste ostrich-and chicken-eggshells as heterogeneous base catalyst for biodiesel production from used cooking oil: Catalyst characterization and biodiesel yield performance. *Applied Energy*, 160 (2015) 58-70.
- [37] K. Seffati, B. Honarvar, H. Esmaili, N. Esfandiari, Enhanced biodiesel production from chicken fat using CaO/CuFe₂O₄ nanocatalyst and its combination with diesel to improve fuel properties. *Fuel*, 235 (2019) 1238-1244.
- [38] Z. Teimouri, A. Salem, S. Salem, Microwave-assisted for clean and rapid fabrication of highly efficient magnetically separable activated carbon from agriculture shells for low grade industrial corn syrup decoloration: A novel strategy for impregnation of ternary catalytic composite. *Food and Bioproducts Processing*, 116 (2019) 78-88.
- [39] S. Niju, J. Indhumathi, K.M.S. Begum, N. Anantharaman, *Tellina tenuis*: a highly active environmentally benign catalyst for the transesterification process. *Biofuels*, 8 (2017) 565-570.
- [40] B.J. Burnett, A. Giles, A.L. Anderson, T. Darger, E. Walker, Rapid Determination of Gold during Plating Operations by Portable X-Ray Fluorescence. *American Journal of Analytical Chemistry*, 5 (2014) 1178.
- [41] F.M. Almutairi, Biopolymer Nanoparticles: A Review of Prospects for Application as Carrier for Therapeutics and Diagnostics. *International Journal of Pharmaceutical Research & Allied Sciences*, 8 (2019).
- [42] S.M. Bahshwan, S.O.A. Rabah, A.M. Turkistani, A comparative study of the effect of crude and nanoparticles *Costus speciosus* on testicular damage associated to experimentally induced type 2 diabetes. *Pharmacophore*, 10 (2019) 99-106.
- [43] N. Mozayeni, A. Morsali, M.R. Bozorgmehr, S.A. Beyramabadi, Structural and mechanistic studies of γ -Fe₂O₃ nanoparticle as troxacitabine drug nanocarrier. *Archives of Pharmacy Practice*, 10 (2019) 31-37.
- [44] H. Babaei, A.A. Sepahy, K. Amini, S. Saadatmand, The Effect of Titanium Dioxide Nanoparticles Synthesized by *Bacillus tequilensis* on *clb* Gene Expression of Colorectal Cancer-causing *Escherichia coli*. *Arch Pharm Pract*, 11 (2020) 22-31.
- [45] J. Gupta, M. Agarwal, Preparation and characterization of CaO nanoparticle for biodiesel production, AIP conference proceedings, AIP Publishing LLC, 2016, pp. 020066.
- [46] E. Bet-Moushoul, K. Farhadi, Y. Mansourpanah, A.M. Nikbakht, R. Molaei, M. Forough, Application of CaO-based/Au nanoparticles as heterogeneous nanocatalysts in biodiesel production. *Fuel*, 164 (2016) 119-127.
- [47] S.L. Lee, Y.C. Wong, Y.P. Tan, S.Y. Yew, Transesterification of palm oil to biodiesel by using waste obtuse horn shell-derived CaO catalyst. *Energy Conversion and Management*, 93 (2015) 282-288.
- [48] A.O. Ayeni, M.O. Daramola, P.T. Sekoai, O. Adeeyo, M.J. Garba, A.A. Awosusi, Statistical modelling and optimization of alkaline peroxide oxidation pretreatment process on rice husk cellulosic biomass to enhance enzymatic convertibility and fermentation to ethanol. *Cellulose*, 25 (2018) 2487-2504.
- [49] Y. Taufiq-Yap, H. Lee, M. Hussein, R. Yunus, Calcium-based mixed oxide catalysts for methanolysis of *Jatropha curcas* oil to biodiesel. *Biomass and bioenergy*, 35 (2011) 827-834.
- [50] M. Kaur, A. Ali, Lithium ion impregnated calcium oxide as nano catalyst for the biodiesel production from karanja and *jatropha* oils. *Renewable Energy*, 36 (2011) 2866-2871.
- [51] H.V. Lee, J.C. Juan, N.F. Binti Abdullah, R. Nizah MF, Y.H. Taufiq-Yap, Heterogeneous base catalysts for edible palm and non-edible *Jatropha*-based biodiesel production. *Chemistry Central Journal*, 8 (2014) 1-9.
- [52] W. Suryaputra, I. Winata, N. Indraswati, S. Ismadji, Waste capiz (*Amusium cristatum*) shell as a new heterogeneous catalyst for biodiesel production. *Renewable Energy*, 50 (2013) 795-799.
- [53] M. Farooq, A. Ramli, A. Naeem, Biodiesel production from low FFA waste cooking oil using heterogeneous catalyst derived from chicken bones. *Renewable Energy*, 76 (2015) 362-368.
- [54] W.N.N.W. Omar, N.A.S. Amin, Optimization of heterogeneous biodiesel production from waste cooking palm oil via response surface methodology. *Biomass and bioenergy*, 35 (2011) 1329-1338.
- [55] M. Zabeti, W.M.A.W. Daud, M.K. Aroua, Biodiesel production using alumina-supported calcium oxide: An optimization study. *Fuel processing technology*, 91 (2010) 243-248.
- [56] O.J. Alamu, O. Dehinbo, A.M. Sulaiman, Production and testing of coconut oil biodiesel fuel and its blend. *Leonardo Journal of Sciences*, 16 (2010) 95-104.
- [57] C. Samart, S. Karnjanakom, C. Chaiya, P. Reubroycharoen, R. Sawangkeaw, M. Charoenpanich, Statistical optimization of biodiesel production from para rubber seed oil by SO₃H-MCM-41 catalyst. *Arabian Journal of Chemistry*, 12 (2019) 2028-2036.
- [58] A. Silitonga, H. Masjuki, H.C. Ong, T. Yusaf, F. Kusumo, T. Mahlia, Synthesis and optimization of *Hevea brasiliensis* and *Ricinus communis* as feedstock for biodiesel production: A comparative study. *Industrial Crops and Products*, 85 (2016) 274-286.
- [59] H. Wu, X. Miao, Biodiesel quality and biochemical changes of microalgae *Chlorella pyrenoidosa* and *Scenedesmus obliquus* in response to nitrate levels. *Bioresource Technology*, 170 (2014) 421-427.
- [60] H. Wu, Y. Liu, J. Zhang, G. Li, In situ reactive extraction of cottonseeds with methyl acetate for biodiesel production using magnetic solid acid catalysts. *Bioresource technology*, 174 (2014) 182-189.
- [61] P. Suwannasom, R. Sriraksa, P. Tansupo, C. Ruangviriyachai, Optimization of biodiesel production from waste cooking oil using waste bone as a catalyst. *Energy Sources, Part A: Recovery, Utilization, and Environmental Effects*, 38 (2016) 3221-3228.

- [62] E. Ajala, F. Aberuagba, A. Olaniyan, M. Ajala, M. Sunmonu, Optimization of a two stage process for biodiesel production from shea butter using response surface methodology. *Egyptian Journal of Petroleum*, 26 (2017) 943-955.
- [63] N. Ghaffari Saeidabad, Y.S. Noh, A. Alizadeh Eslami, H.T. Song, H.D. Kim, A. Fazeli, D.J. Moon, A review on catalysts development for steam reforming of biodiesel derived glycerol; Promoters and supports. *Catalysts*, 10 (2020) 910.
- [64] A. Lee, N. Chaibakhsh, M.B.A. Rahman, M. Basri, B.A. Tejo, Optimized enzymatic synthesis of levulinate ester in solvent-free system. *Industrial Crops and Products*, 32 (2010) 246-251.
- [65] E. Ajala, F. Aberuagba, A. Olaniyan, M. Ajala, M. Sunmonu, Optimization of a two stage process for biodiesel production from shea butter using response surface methodology. *Egyptian Journal of Petroleum*, 26 (2017) 943-955.
- [66] D. Leung, Y. Guo, Transesterification of neat and used frying oil: optimization for biodiesel production. *Fuel processing technology*, 87 (2006) 883-890.
- [67] S.A. Razack, S. Durairasan, Response surface methodology assisted biodiesel production from waste cooking oil using encapsulated mixed enzyme. *Waste Management*, 47 (2016) 98-104.
- [68] K. Shah, K. Maheria, J. Parikh, Effect of reaction parameters on the catalytic transesterification of cottonseed oil using silica sulfuric acid. *Energy Sources, Part A: Recovery, Utilization, and Environmental Effects*, 38 (2016) 1470-1477.
- [69] S. Oko, I. Syahrir, M. Irwan, The Utilization of CaO Catalyst Impregnated with KOH in Biodiesel Production from Waste Cooking Oil. *Int. J. Sci. Technol. Res.*, 7 (2018) 115-118.
- [70] N.S. Lani, N. Ngadi, N.Y. Yahya, R. Abd Rahman, Synthesis, characterization and performance of silica impregnated calcium oxide as heterogeneous catalyst in biodiesel production. *Journal of Cleaner Production*, 146 (2017) 116-124.
- [71] Y. Dallatu, E. Agbaji, V. Ajibola, The influence of physicochemical characteristics of a non-edible oil of yellow oleander seed on its fuel properties. *Bayero Journal of Pure and Applied Sciences*, 10 (2017) 283-291.
- [72] N. Siatas, A. Kimbaris, C. Pappas, P. Tarantilis, M. Polissiou, Improvement of biodiesel production based on the application of ultrasound: monitoring of the procedure by FTIR spectroscopy. *Journal of the American Oil Chemists' Society*, 83 (2006) 53-57.
- [73] J. Omowanle, R. Ayo, J. Habila, J. Ilekhaize, E. Adegbe, Physico-chemical and Gc-MS Analysis of some selected plant seed oils; Castor, Neem and Rubber Seed Oils. *FUW Trends Sci. Technol. J.*, 3 (2018) 644-651.
- [74] P.W. Mwaurah, S. Kumar, N. Kumar, A. Panghal, A.K. Attkan, V.K. Singh, M.K. Garg, Physicochemical characteristics, bioactive compounds and industrial applications of mango kernel and its products: A review. *Comprehensive Reviews in Food Science and Food Safety*, 19 (2020) 2421-2446.
- [75] C. Dorni, P. Sharma, G. Saikia, T. Longvah, Fatty acid profile of edible oils and fats consumed in India. *Food chemistry*, 238 (2018) 9-15.
- [76] H. Darmstadt, C. Roy, S. Kaliaguine, S. Choi, R. Ryoo, Surface chemistry of ordered mesoporous carbons. *Carbon*, 40 (2002) 2673-2683.
- [77] A. Warra, F. Sheshi, H. Ayurbami, A. Abubakar, Physico-chemical, GC-MS analysis and cold saponification of canary melon (*Cucumis melo*) seed oil. *Trends in Industrial Biotechnology Research*, 1 (2015) 10-17.
- [78] R. Piloto-Rodríguez, Y. Sánchez-Borroto, M. Lapuerta, L. Goyos-Pérez, S. Verhelst, Prediction of the cetane number of biodiesel using artificial neural networks and multiple linear regression. *Energy Conversion and Management*, 65 (2013) 255-261.
- [79] G. Knothe, R.O. Dunn, M.O. Bagby, Biodiesel: the use of vegetable oils and their derivatives as alternative diesel fuels, ACS symposium series, Washington, DC: American Chemical Society, [1974]-, 1997, pp. 172-208.
- [80] J. Alademeyin, J. Arawande, Physicochemical properties and fatty acid composition of crude and processed *Adenopus breviflorus* Benth seed oil. *Bangladesh Journal of Scientific and Industrial Research*, 51 (2016) 159-166.
- [81] W. Institute, Biofuels for transport: global potential and implications for sustainable energy and agriculture, Earthscan(2012).
- [82] C. Beaudoin-Chabot, L. Wang, A.V. Smarun, D. Vidović, M.S. Shchepinov, G. Thibault, Deuterated polyunsaturated fatty acids reduce oxidative stress and extend the lifespan of *C. elegans*. *Frontiers in physiology*, 10 (2019) 641.
- [83] M. Oseni, S. Obeta, F. Orukotan, Evaluation of fatty acids profile of ethyl esters of yellow oleander and groundnut oils as biodiesel feedstock. *Am. J. Sci. Ind. Res.*, 3 (2012) 62-68.
- [84] U. Rashid, F. Anwar, G. Knothe, Evaluation of biodiesel obtained from cottonseed oil. *Fuel Processing Technology*, 90 (2009) 1157-1163.